Ph.D. thesis

Development of directly compressible

ambroxol hydrochloride spherical crystals

Orsolya Gyulai

Szeged

2018

University of Szeged

Faculty of Pharmacy

Institute of Pharmaceutical Technology and Regulatory Affairs
Head: Dr. habil. Ildikó Csóka Ph.D.

Development of directly compressible ambroxol

hydrochloride spherical crystals

Ph.D. thesis

Orsolya Gyulai
Chemist

Supervisor:
Dr. habil. Zoltán Aigner Ph.D.

Szeged
2018

Table of contents

List of original publications

I.   Gyulai, O.; Szabó-Révész, P.; Aigner, Z.:
Comparison study of different spherical crystallization methods of ambroxol hydrochloride
Cryst. Growth Des. 2017, 17 (10), 5233-5241
DOI: 10.1021/acs.cgd.7b00764   **IF: 4.055**

II.   Gyulai, O.; Kovács, A.; Sovány, T.; Csóka, I.; Aigner, Z.:
Optimization of the critical parameters of the spherical agglomeration crystallization method by the application of the Quality by Design approach
Materials 2018, 11(4), 635
DOI: 10.3390/ma11040635   **IF: 2.654**

III.   Gyulai, O.; Aigner, Z.:
A szférikus kristályosítás típusai, jelentősége a gyógyszeriparban
Acta. Pharm. Hung. APHGAO 2018, 88(043), 17-26   **IF: 0.00**
ISSN: 0016659

IV.   Gyulai, O.; Aigner, Z.:
On-line observation of the crystal growth in the case of the non-typical spherical crystallization methods of ambroxol hydrochloride
Powder Technol. 2018, 336 C, 144-149
DOI: 10.16/j.powtec.2018.05.041   **IF: 2.942**

Abstracts

1) The structure of tin(II) in strongly alkaline aqueous solutions; E. Czeglédi, É. G. Bajnóczi, Orsolya Gyulai, István Pálinkó, Gábor Peintler, Ottó Berkesi, Ernő Kuzmann, Zoltán Homonnay, Pál Sipos; Recent developments in coordination, bioinorganic, and applied inorganic chemistry – Monograph series of the International Conferences on Coordination and Bioinorganic Chemistry, Vol. 11, pg. 14-19, Smolenice, 2013

2) Az Sn(II)- és Pb(II)-ionok viselkedése erősen lúgos közegben; Gyulai Orsolya, Bajnóczi Éva, Sipos Pál, Pálinkó István; XXXVII. Kémiai Előadói Napok, Program- és előadás-összefoglalók; ISBN 978-963-9970-53-3, Szeged, 2014

3) Synthesis of azide−CaAl-LDH nanocomposite by an improved mechanochemical procedure, Orsolya Gyulai, Márton Szabados, Pál Sipos, István Pálinkó; NANO Ostrava Konferencia, Konferenciakiadvány, ISBN 978-80-248-3745-1, pg. 121, Ostrava, 2015

4) Az ambroxol-hidroklorid szférikus kristályosításához szükséges paraméterek beállítása, Gyulai Orsolya, Aigner Zoltán; MKE Kristályosítási és Gyógyszerformulálási Szakosztály, 9. Kerekasztal Konferencia programfüzet, pg. 13, Balatonszemes, 2016

5) Spherical crystallization methods of ambroxol hydrochloride; Orsolya Gyulai, Piroska Szabó-Révész, Zoltán Aigner; 5th International School of Crystallization, Conference Proceedings, pg. 120, Granada, 2016

6) Refining the parameters of spherical crystallization methods, Orsolya Gyulai, Piroska Szabó-Révész, Zoltán Aigner; BIWIC 2016 – 23rd International Workshop on Industrial Crystallization, Conference Proceedings, pg. 246-251, Magdeburg, 2016

7) Az ambroxol-hidroklorid szférikus kristályosításának módszerei, Orsolya Gyulai; Clauder Ottó Emlékverseny programfüzet, pg. 23, Budapest, 2016

8) A szférikus agglomeráció paramétereinek optimalizálása faktoriális kísérleti terv alapján, Gyulai Orsolya, Aigner Zoltán; MKE Kristályosítási és Gyógyszerformulálási Szakosztály, 10. Kerekasztal Konferencia programfüzet, pg. 29, Balatonszemes, 2017

9) Optimization of the parameters of spherical agglomeration, Orsolya Gyulai, Zoltán Aigner; FIP PSWC 2017 – Pharmaceutical World Congress, Stockholm, 2017

10) Optimization of the parameters of spherical agglomeration, Orsolya Gyulai, Zoltán Aigner; ECS 4 – 4th European School of Crystallography, Book of Abstracts, pg. 41-42, Warsaw, 2017

11) Parameter optimization of the spherical agglomeration method, Orsolya Gyulai, Anita Kovács, Tamás Sovány, Ildikó Csóka, Zoltán Aigner; BBBB Conference, Acta Pharmaceutica Hungarica, 2017, 3-4., APHGAO 87, (043) 85-244. (2017), pg. 143 (P1C-1), Balatonfüred, 2017

12) Optimization of the parameters of the spherical agglomeration method, Orsolya Gyulai, Zoltán Aigner; ICG 2017 – Italian Crystal Growth Abstracts Book, pg. 67-68, Milano, 2017

13) Közvetlen préselésre alkalmas szférikus kristályok előállítása, Gyulai Orsolya, Aigner Zoltán; MKE Kristályosítási és Gyógyszerformulálási Szakosztály, 11. Kerekasztal Konferencia programfüzet, pg. 16-17, Balatonszemes, 2018

14) Following crystal growth with the help of FBRM technique in case of ambroxol hydrochloride spherical agglomerates; Orsolya Gyulai, Zoltán Aigner, 9th Global Chemistry Congress, Conference Proceedings, pg.   , Lisbon, 2018

Abstract

Abbreviations

AMB HCl	Ambroxol hydrochloride
API	Active Pharmaceutical Ingredient
ATP	Slow cooling crystallization with alternating temperature profile
CMAs	Critical material attributes
CPPs	Critical process parameters
CQAs	Critical quality attributes
DMSO	Dimethyl sulfoxide
DoE	Design of Experiments
DS	Design Space
DSC	Differential scanning calorimetry
EtOH	Ethanol
FD	Factorial design
ICH	International Conference on Harmonization
IPA	Isopropyl alcohol
MeOH	Methanol
MSZW	Metastable zone width
REM	Risk estimation matrix
SA	Spherical agglomeration
SEM	Scanning electron microscopy
TG	Thermogravimetry
QbD	Quality by design
QESD	Quasi-emulsion solvent diffusion method
QTPPs	Quality target product profile
W	Purified water
XRPD	X-ray powder diffractometry

1.   Introduction

Manufacturing spherical crystals [1, 2] with appropriate particle size is an important objective for APIs dedicated to direct tablet making. The material chosen for our experiments, ambroxol hydrochloride (AMB HCl), is such a solid compound. The optimal habit for the crystals of direct compressible active agents and additives includes spherical morphology, proper mean particle size and appropriate surface.[3]

These parameters can determine the powder rheological attributes of the crystalline material.[4, 5] The ones with good flowing, compaction and compression properties are suitable for the direct compression tablet making method, which is a more economical way of producing tablets and also has several advantages compared to the basic tableting methods containing granulation process.[6-8] It can also be applied to moisture sensitive compounds, since it is a simple, one-step process without the use of any granulation liquids. With the help of this method, amount of additives can be reduced, therefore, smaller tablets with the same drug dose can be manufactured, improving the patient compliance.[9]

However, spherical crystallization can be really difficult to accomplish. Not only the finding of the suitable method can be a long and time-consuming process, but also the finding of the appropriate solvents, antisolvents and bridging liquids. Once the proper production method is found, parameter optimization is also indispensable, for which, quality tools are usually used. On the basis of Quality by Design (QbD) fundamentals, risk assessment can be carried out, which is an important step in case of industrial operations. This way, process control can be more effective and the whole production becomes more economical.

2.   Aims

Process development is present in all fields of industrial production. In this work, the following bullet points were desired to accomplish:

- to apply and compare the typical and the non-typical spherical crystallization methods in the case of the chosen model drug, AMB HCl;
- to designate the process resulting spherical particles, the parameters of which match our requirements the best and investigate the powder rheological attributes of this crystalline material;
- to optimize the parameters of the chosen methods;
- to carry out a risk assessment and then optimize the parameters of the spherical agglomeration method based on the quality by design principles;
- to observe the non-typical crystallization methods with focused beam reflectance measurement and to optimize the parameters of the slow cooling crystallization method with an alternating temperature profile based on the results of the real-time measurements.

3.   Literature survey

3.1.   Direct compression tablet making

It is well known, that crystallization is the last step in the production of solid form active pharmaceutical ingredients (APIs) and additives. It is suitable not only for purification but also for obtaining the proper crystal size and morphology.[10, 11] Particle size, surface and distribution can influence many attributes of crystalline materials and are valuable indicators of quality.[12] The particle size (also its distribution) and shape influence flow and compaction properties.[13-15]

Particle size is a well-known determinant of dissolution with smaller particles dissolving faster, thus, methods of particle size reduction have been in the focus of pharmaceutical technological research in the past decade, especially in case of materials with low water solubility.[16, 17] However, larger and spherical-like particles are typically characterized by a better flowability compared to smaller particles with a high aspect ratio, thus, the former are more suitable for direct compression experiments to identify the most suitable method for obtaining crystals for direct compression tableting method ($80 \ \mu m <$ size range $< 1000 \ \mu m$ [18, 19]; roundness, aspect ratio $\rightarrow 1.00$). Generally, it can be said, that a slow crystallization process with low supersaturation results in larger crystals.[20] Enlargement of particle size of several drug materials can be accomplished by spherical crystallization, for example, magnesium aspartate, acetylsalicylic acid [21-23], paracetamol [24] and ibuprofen [25]. Large and good-flowing particles are also better for encapsulation.[26]

One of the advantages of applying direct compression for a crystalline API is the avoidance of granulation [27], which is a time- and money-consuming process from an industrial point of view.[28] It is also beneficial when the API or the excipients are thermolabile or moisture-sensitive. Large-size, spherical or plate-shaped crystals are the favorable in order to improve the flowability, compactibility, and compressibility of the API.[29-32] Producing spherical crystals suitable for direct tableting allows the amount of additives to be reduced, thus tablet size can be decreased, facilitating swallowing.[33] It is known that modifying the solvents and the conditions applied for the crystallization process affects particle size and morphology.[34, 35]

AMB HCl was chosen for our experiments because no other research has been reported on the crystallization of this API yet, although it is known that direct

compression is the readily accepted method for the preparation of ambroxol tablets.[36, 37] This API usually crystallizes as a fine powder, (< 20 μm) which means, that it is cohesive, thus unfavorable for direct compression tablet making. This API is the salt form of ambroxol, the metabolite of bromhexine. It is an expectorant with mucokinetic and secretolytic properties used in the treatment of common cold and cough, bronchial asthma and chronic bronchitis and even inhibits human rhinovirus.[38-41]

3.2. Types of spherical crystallization

Two main types of spherical crystallization procedures are distinguished: typical and non-typical ones. Usually, there are three solvents in typical spherical crystallization methods, namely a good solvent, an antisolvent and a bridging liquid which is miscible with the other two and also wets the active agent.[42-45] Emulsifiers are also used for this technique to stabilize the emulsion droplets and to maintain a homogeneous droplet size. [46] The most well-known typical spherical crystallization method is quasi-emulsion solvent diffusion technique.[5, 47-52]

Only one solvent phase is present in case of non-typical spherical crystallization methods such as spherical agglomeration, which is an antisolvent technique [53-55], or programmed cooling crystallization [56-60] (or a combination of these [61, 62]). With the help of an alternating temperature profile during cooling, particle size distribution can be standardized, thus when the system is heated up, smaller particles dissolve while the larger particles decrease in size and their roundness improves. Then, during the solution's cooling phase, new particles crystallize onto the surface of these still larger but rounder particles. Seeding is a very important moment in this case because the main aim of the process is to keep the number of the particles almost constant by the enlargement of the seeding particles.[63, 64]

3.3. Importance of polymorphism

Not only crystal morphology, but polymorphism is also a critically important parameter which can be modified by the use of different types of solvents and solvent mixtures. In the field of crystallization, the exact polymorphic forms always have to be identified and described, because different forms can have different physical and physicochemical properties such as solubility.[65] AMB HCl has got one

known polymorphic form which has got the same XRPD pattern as our samples and its crystal structure is C2/c, monoclinic.[66]

3.4. Quality by design and risk assessment

Before applying new technologies, it is really important to carry out a risk assessment in industrial production either it is pharmaceutical industry or any other field. Wrongly-selected critical parameters can affect the product in an unprofitable way, which can cause great loss. The application of the QbD methodology according to the ICH Q8 and Q9 guidelines [67, 68] is a fairly new approach in the development phase of new pharmaceutical products.[69-71] The QbD concept is a systematic process for the assessment, control, communication and review of risks to the quality of the active pharmaceutical ingredients through the product lifecycle. The QbD concept provides scientific product development, which involves the identification of the quality target product profile (QTPP) defining critical quality attributes (CQAs), critical material attributes (CMAs) and critical process parameters (CPPs), using risk assessment and optimization of data analysis with the use of design of experiments (DoE).[72] Several quality management tools can be found in the ICH guideline Q9, for example, Pareto analysis, Ishikawa diagram, risk estimation matrix (REM). On the basis of the results of the risk assessment, which shows the critical parameters of the procedure, a factorial design can be applied which is a simple method for screening out the optimal parameter-combination.[73, 74] Risk assessment aims at identifying which material attributes and process parameters potentially influence the product CQAs, furthermore, they can help to obtain all the significant factors which will be subjected to the DoE study to establish product and process design space (DS).[75-77]

3.5. Importance of real-time observation methods

Possessing facilities for the use of on-line or in-line imaging or particle size-observing methods, a real-time tracking of nucleation and crystal growth can be achieved. The focused beam reflectance measuring method (FBRM) is a modern and accurate method for in-line or even on-line measurements.[78] Pioneers of this topic - among others - were *Sohrab Rohani, Marco Mazotti, Sotiris E. Pratsinis, Brian Glennon* and *Zoltán Nagy K. Rohani et. al.* initiated measurements with the help of turbidimetry and they were able to indicate approximately the beginning of the

crystallization mechanism and describe the average particle size both experimentally and based on theoretical calculations.[79] *Mazotti* and his co-workers analyzed in-situ microscopic data and described a method that can be applied in the prediction of experimental data.[80] Later they also used the FBRM for particle size distribution control.[81] *Pratsinis* and his co-workers have in-situ measured the crystal growth and size and of nanoparticles.[82] *Brian Glennon* and his colleagues investigated the effect of the probe position and orientation on particle size in dilute agitated suspensions. They have also predicted theoretically the normalized chord length distribution values and these correlated well with the results of the FBRM measurements.[83] *Zoltán Nagy K. et. al.* also used non-invasive particle size observation methods as on-line techniques for crystallization and applied an alternating temperature profile during cooling crystallization, so the mean particle size and its distribution could be standardized (CryPRINS program).[84]

4. Materials

AMB HCl was generously supplied by TEVA Pharmaceutical Industries Ltd. (Hungary). All the applied solvents were of analytical grade. Dimethyl sulfoxide (DMSO) and *n*-hexane were purchased from Scharlau Concept Co., Ltd. (Hungary). Ethyl acetate, isopropyl alcohol (IPA), *n*-pentane *n*-heptane and *n*-dodecane were purchased from Molar Chemicals Ltd. (Hungary), methanol (MeOH) and ethanol (EtOH) were purchased from VWR Hungary. Isopropyl acetate was purchased from Brenntag Hungary Ltd. Purified water (W) of Ph. Eur. quality was used for the experiments. Span 80, Tween 20, Span 80 and Span 20 were Sigma-Aldrich products. Purified water and methanol for the FBR measurements were supplied by EGIS Pharmaceuticals Plc. All the applied solvents were of analytical grade.

5. Methods

5.1. General information

A Julabo F32-ED Refrigerated/Heating Circulator® was used for setting and keeping the required temperature during the crystallization processes and the solubility measurements. Drying of the crystals was carried out with a Memmert dry heat sterilizator at 40 °C. Determination of the metastable zone width and the on-line observations were carried out with a Mettler Toledo FBRM D600R probe (and the temperature was controlled with a Huber Petite Fleur Pilot ONE thermostat. The average number of particles (for each size range) was followed by the iContol FBRM 4.3.377 (Columbus, Ohio, USA) controller software.

5.2. Determination of solubility

Determination of the solubility of AMB HCl was necessary because the appropriate solvents had to be assigned to each crystallization method. It determined by the gravimetric method [85] in pure MeOH, EtOH, IPA, W and in mixtures of different volume ratios of W/MeOH, W/EtOH and W/IPA (1:1, 1:3, 3:1 each). The temperature range was 25-65 °C and three parallel measurements were carried out. For each measurement it took 24 hours to reach the equilibrium, then mixing was stopped to allow the suspended solid phase to settle down and afterward the clear solution was sampled into a vessel with a known mass.

5.3. Crystallization utilizing typical methods

5.3.1. Quasi-emulsion solvent diffusion technique (QESD)

AMB HCl was found to have the two highest solubility values in W/MeOH = 1:3 mixture and W/EtOH = 1:3 and 1:1 mixtures, therefore these were used as good solvents. The bridging liquid was MeOH and EtOH, respectively, since these are miscible with both the solvent and the antisolvent and they wet the active agent well. As antisolvents ethyl acetate, isopropyl acetate, *n*-pentane, *n*-hexane, *n*-heptane, and *n*-dodecane were used. A solvent/antisolvent ratio of 1:5 was applied based on literature data.[86] The effects of different types and amounts of emulsifiers were also investigated using mixtures of Span 80/Tween 20 and Span 80/Span 20, setting an

9

HLB (hydrophilic-lipophilic balance [87]) value that contributes to the most stable emulsion and gives the highest yield.

$$HLB_{total} = Weight\%_1 \cdot HLB_1 + Weight\%_2 \cdot HLB_2$$

Different amounts of emulsifiers were added to the antisolvent, followed by the dropwise addition of the saturated solutions of AMB HCl besides constant mixing with a magnetic stirrer at 25 °C for about 24 hours while the crystallization process took place. A 150 ml jacketed crystallization vessel was applied with a total solvent volume of 60 ml.

5.4. Crystallization utilizing non-typical methods

5.4.1. Spherical agglomeration (SA)

Nearly-saturated solutions of AMB HCl were prepared using MeOH, W/EtOH = 1:1 and 1:3 mixtures and DMSO as solvents, respectively. Ethyl acetate, isopropyl acetate, *n*-pentane, *n*-hexane, and *n*-heptane were applied as antisolvents. The effects of various volume ratios of the solvent and the antisolvent were examined. The applied ratios were 1:2, 1:5, and 1:10. In each case, the nearly-saturated AMB HCl solution was added into the antisolvent dropwise and then left for 24 hours to crystallize at 25 °C in a total volume of 50 ml. A 150 ml jacketed crystallization vessel was applied during the process, and the system was gently agitated.[88]

5.4.2. Slow cooling with an alternating temperature profile (ATP)

A nearly-saturated solution of AMB HCl (in W/MeOH = 1:3 solvent) at 60 °C was repetitively cooled and warmed back around the metastable zone. The system was investigated in a 250 ml double-walled vessel in a total solvent volume of 70 ml. The appropriate cooling-heating program starts from 70 °C in order to make sure that every single particle was dissolved. Then the gradual cooling (- 0.3 °C/min) of the solution was started until around 50 °C when seeding crystals were fed into the system. Next, the solution is gradually cooled to 30 °C and warmed back to 50 °C (+ 0.3 °C/min). This step is repeated until the sample was cooled to 10 °C.

5.5. Determination of the metastable zone

Determination of the metastable zone width (MSZW) is useful before starting any experiments because this property of the material can unfavorably affect the

crystallization procedure. It was carried out in a Schmizo AG (Oftringen, Switzerland) jacketed glass reactor of 500 ml, equipped with a Mettler Toledo FBRM D600R probe (Columbus, Ohio, USA) and the temperature was controlled with a Huber Petite Fleur Pilot ONE thermostat (Old Town, Maine, USA). Five different concentrations of AMB HCl solutions (in W/MeOH = 1:3 solvent) were used for the experiments. The solubility experiments provided information on the saturation temperatures. The cooling rate was 0.3 °C/min, similarly to the crystallization procedures. The baseline temperature for the experiment was 70 °C to make sure that no solid particles are present in the solution saturated at 60 °C. The cooling program was linear to the metastable point at which additional solvent was fed into the vessel to start the next measurement at a different concentration and temperature scenario.

5.6. Risk assessment

5.6.1. Definition of the QTPP and determination of CQAs, CMAs and CPPs

The first step of carrying out process development by the QbD approach is defining QTPPs. These are quality, safety and efficiency features of a product, for example, the dosage form, the route of administration, etc. As a second step, defining the quality attributes of the product is necessary. The CQAs are derived from the QTPP and prior product knowledge. In pharmaceutical development, the CQA is usually a physical, chemical, biological, or microbiological property. The next step is to determine the material attributes and process parameters that may influence the CQAs. These factors were designated on the basis of literature data, pilot experiments and personal experiences.

5.6.2. Quality tools

The following quality tools were applied during the risk assessment: Ishikawa diagram and Pareto analysis. Once the predominant causes are identified, tools like the Ishikawa diagram can be applied to identify the root causes of a problem.[89-92] The Pareto analysis represents the correlations between CPPs and CQAs and it can show us the most critical parameters which have to be paid attention to during development.[93-95] This technique helps the identification of the critical parameters

that can influence a process.[89, 94, 96] LeanQbD Software (Version 1.3.6., 2014, QbD Works LLC) is used for the evaluation of risk severity scores.

5.6.3. Factorial design

After the evaluation of the risk assessment, the dependent and the independent variables of the following factorial design (FD) can be defined. The levels of the factors have to be determined and, as a next step, crystallization needs to be carried out with the previously-described factors. As a result, dependent variables could be measured and Statistica 13 for Windows program was then used for the statistical evaluation. In a factorial experiment all levels (n) of a given factor (m) are combined with all levels of every other factor included in the experiment, and the total number of experiments is "$n \cdot m$".[97] As in this case a 2-3 mixed-level factorial design was used, 36 experiments were planned and, on the basis of the coefficients, polynomial correlations were defined and the significance of the factors was determined.

5.7. SA method for parameter optimization

This technique was described and applied in our previous research (SA method for parameter optimization).[98] Since many of the process parameters were considered as key parameters during the SA method, it was further perfectionated via applying a factorial design to it, which was based on the results of a previous risk assessment. DMSO was chosen as a solvent and ethyl acetate was the antisolvent in their 1:5 ratio. The saturation of the solution was 440 mg/ml. The temperature difference between the solvents (dT) was set and then the nearly-saturated solution was fed into the antisolvent besides agitation. Agitation was carried out with a Heidolph Titramax 101 horizontal shaker (Schwabach, Germany) set to 150 rpm. The crystals were produced in a double-walled vessel in the volume of 78 ml, 7 cm width and 10 cm length. These geometrical parameters were important in the regards to the column height of the solution and thus, the effect of the agitation. After crystallization with the chosen parameters, the products were separated by vacuum filtration and washed with 10 ml of ethyl acetate, then dried at 40 °C for 24 hours.

5.8. Non-typical crystallization methods for on-line measurements

5.8.1. SA method

During this method, four products of the SA method for parameter optimization with the best average size, roundness and aspect ratio values were prepared by applying two different process sets. SA 1 experiments were carried out in a rounded-bottomed jacketed reactor (250 ml) in a total volume of 78 ml, while for SA 2 experiments, a Schmizo jacketed glass reactor (750 ml), also with a rounded bottom, was applied with a total solvent volume of 500 ml. In each case, a nearly-saturated solution of the API was fed in the antisolvent dropwise. For agitation, a horizontal shaker (for SA 1 experiments) and a marine propeller (for SA 2 experiments) were applied with 150 and with 250 rpm agitation speeds. In the first section of the crystallization process, 150 rpm was applied because, based on pre-experiments, lower agitation rate in the critical crystal formation section yields larger average particle size. However, for the execution of the on-line measurement, a higher agitation rate was necessary to provide a higher flow-rate and better perceptibility. The applied process parameters are summarized in Table 1, based on the results of the parameter optimization.

Table 1. The applied parameters during the experiment set, SA. Column dT means the temperature difference between the solvent and the antisolvent.

Sample name	Mixing time (min)	dT (°C)
SA 1-2 A	30	0
SA 1-2 B	90	0
SA 1-2 C	30	10
SA 1-2 D	90	10

5.8.2. ATP method

W/MeOH mixture (ratio 1:3) was chosen as a solvent, which was saturated with the API at 60 ºC. ATP 1 experiments were carried out in a jacketed reactor (250 ml) in a total volume of 120 ml, while for ATP 2 experiments a Schmizo jacketed glass reactor (750 ml) was applied. Horizontal shaker was applied for the ATP 1 experiments and marine propeller for the ATP 2 experiments. In both cases, a controlled, cyclic cooling-heating program was applied with ± 0.3 ºC/min heating-cooling rate, based on the pre-experiments describing the metastable zone. The agitation rate was 250 rpm.

5.9. Product assays

5.9.1. Light microscopy

Images were taken with a JVC digital camera connected to the microscope and the computer. Image J program was used for the installation of scale bars.

5.9.2. Mean particle size, particle size distribution, roundness and aspect ratio

For the determination of mean particle size (d50, D[1,0]) and particle size distribution, aspect ratio and roundness a LEICA Q500 MC Image Processing and Analysis System (Wetzlar, Germany) was used, measuring at least 1000 particles. Because of the small amounts of samples analyzed, this equipment is more suitable than a laser diffraction-based particle size analyzer as this one can provide specific information on individual particles (for example individual roundness values).

The shape factor, "roundness" gives a minimum value of 1.00 for a sphere. It is calculated from the ratio of the perimeter squared to the area as follows:

$$Roundness = \frac{Perimeter^2}{4 \cdot \pi \cdot Area \cdot 1.064}$$

The adjustment factor of 1.064 corrects the perimeter for the effect of the corners produced by the digitization of the image.[16] "Area" is the area of one pixel multiplied with the detected number of pixels.

Aspect ratio is the length divided by the width of the particle. This parameter is calculated from the average length and width values and it describes the shape of the particle. For spheres, it is 1.00, such as roundness.

5.9.3. Scanning electron microscopy

The morphology of the particles was examined by SEM (Hitachi S4700, Krefeld, Germany). A sputter coating apparatus (Bio-Rad SC 502, Microtech, England) was applied to induce electric conductivity on the surface of the samples. Air pressure was 1.3-13.0 mPa.

5.9.4. Polymorphism

X-ray Powder Diffractometry (XRPD)

The diffractograms were collected with a BRUKER D8 Advance diffractometer (Karlsruhe, Germany) system equipped with a Våntec 1 line detector (Karlsruhe, Germany) with Cu $K_{1\alpha}$ radiation (= 1.5406 Å) over the interval 3-40° 2θ, using

40 kV and 40 mA with rotation switched on. The measurement conditions were as follows: filter, Ni; time constant, 0.1 s; angular step 0.007°, sample holder: Si low background sample holder.

Differential Scanning Calorimetry (DSC)

The DSC curves were collected with a Mettler Toledo DSC 821^e apparatus (Columbus, Ohio) within the temperature interval of 25-300 °C with an Ar gas intake of 10 l/h. Heating was linear with a heating rate of 10 °C/min. The masses of the samples were between 2 and 5 mg in a 40 µl Al pinned crucible with lid.

Thermogravimetry (TG)

The TG curves were collected with a Mettler Toledo TGA/DSC 1 STAR^e System (Columbus, Ohio) within the temperature interval of 25-300 °C with an N_2 gas intake of 10 l/h. Heating was linear with a heating rate of 10 °C/min. The masses of the samples were between 9 and 12 mg in a 100 µl Al sample holder.

5.9.5. Powder rheology tests

Flow time, the angle of repose and bulk density were measured with Pharma Test PTG-1 Powder Characterization Instrument (Hainburg, Germany), with Teflon funnel and with the manual method written in the VII. Hungarian Pharmacopoeia [99] with a glass funnel. Three parallel measurements were carried out. Bulk and tapped densities were determined by the STAV 2003 Stampfvolumeter (Ludwigshafen, Germany) and based on the results Carr index and Hausner factor were calculated.

5.9.6. Mechanical strength test

The mechanical strength of the crystal agglomerates was numerically characterized by an individually-developed mechanical strength tester apparatus [100] and the associated computer software that is able to visually display the fracture curve. This instrument measures the force applied for the fracture of the particles or pellets that are put under the breaking head. We broke 20 particles for each measurement.

5.9.7. Residual solvent content

The residual solvent content was determined by the headspace gas chromatographic method using an Agilent 7890B PAL RSI85 apparatus equipped with a Shimadzu 2010 Plus AOC-5000 headspace injection system.

6. Results and discussion 1 – Comparison of the spherical crystallization methods

6.1. Solubility of ambroxol hydrochloride in different solvents

The solubility of AMB HCl was measured in mixtures of W/EtOH, W/MeOH, and W/IPA, so was in the pure solvents. The solubility curves are shown in Fig. 1. Experiments were also carried out in *n*-pentane, *n*-hexane, and *n*-heptane. The solubility in these liquids was ~ 0 mg/ml, therefore these seemed to be good antisolvents.
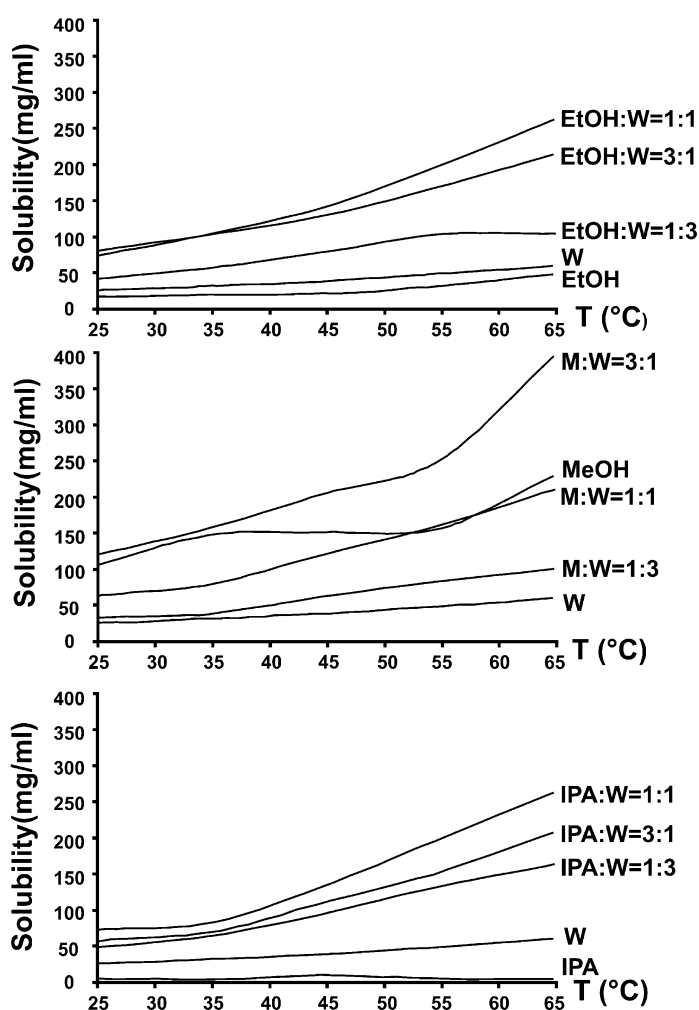
Fig. 1. Solubility of AMB HCl in water, different alcohols and water-alcohol mixtures

The solubility of AMB HCl was low (< 30 mg/ml) in water and even in EtOH at ambient temperature. In apolar solvents such as *n*-heptane, *n*-hexane, *n*-pentane the solubility of AMB HCl was negligibly low. Its solubility was similarly low but measurable in isopropyl and ethyl acetate (< 0.5 mg/ml), thus all of these may serve

as optimal antisolvents. DMSO (> 400 mg/ml) and MeOH (> 110 mg/ml) were proven to be good solvents for AMB HCl. DMSO was chosen to be the good solvent for the SA procedure since high saturation could be achieved with it. W/EtOH (1:1) and W/MeOH (1:3) mixtures were chosen for the ATP and the QESD methods. The water/alcohol mixtures could serve as good solvents for the typical method because these systems have a co-solvent effect as the mixtures dissolve more API than the pure solvents alone. Therefore, when alcohol diffuses out of the emulsion droplet, solubility decreases inside promoting crystallization. This characteristic is optimal when the metastable zone is narrow.

6.2. Determination of the metastable zone

As a temperature- and solution-dependent parameter, the metastable zone is highly important in case of cooling crystallization. However, it is also relevant for the QESD method that was carried out using the same solvent mixture at 25 °C. The metastable zone for AMB HCl using W/MeOH = 1:3 solvent mixture is shown in Fig. 2.
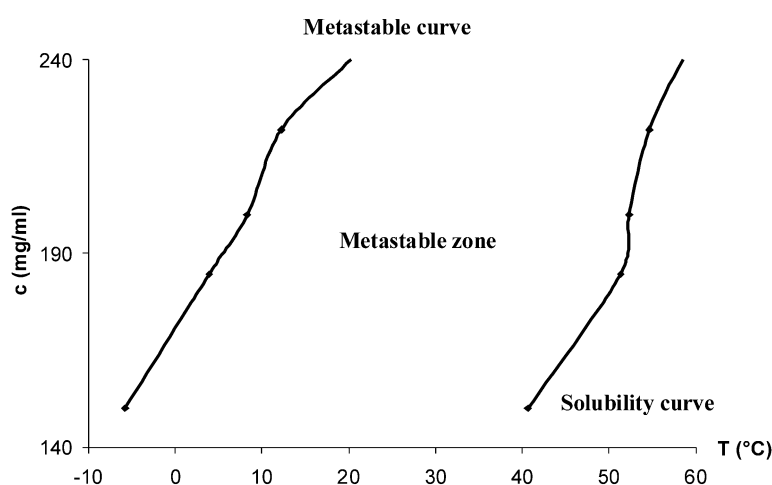
Fig. 2. Metastable zone of AMB HCl in W/MeOH = 1:3 solvent

In our case the metastable zone was obviously wide, thus spontaneous nucleation may occur only at lower temperatures. Once it happens, crystallization is always a fast process which is disadvantageous in terms of particle size enlargement. Therefore, in our subsequent experiments of ATP method, we applied a tightly restricted seeding procedure in the temperature interval assigned to lower

supersaturation values, in order to prevent a fast and spontaneous crystallization and rather promote a slow crystallization process yielding large crystals.

6.3.   Crystallization utilizing typical methods: QESD method

Determination of the parameters of QESD method starts with trying out several solvent systems and decides which worked best, followed by the exchange of the type and the amount of the emulsifiers. Based on the literature, an HLB value of 7.3 is suitable for this type of crystallization incorporating a similar solvent system, but a different type of solid material. [86] In our case, the same HLB value seemed to be the best on the basis of visual observations and product yield in preliminary experiments. Fig. 3. shows the effect of the solvent system on crystal size and morphology. It was revealed that the modification of the solvent system can induce significant differences in crystal morphology and size. For the sample on Fig 3A (QESD 1) a W/MeOH = 1:3 mixture was used as a good solvent, n-heptane as the antisolvent and MeOH as the bridging liquid. For the sample on Fig 3B (QESD 2) MeOH was used as a good solvent and n-pentane as the antisolvent. In both cases one drop of a Span 80/Tween 20 emulsifier mixture was used for a total solvent volume of 15 ml.
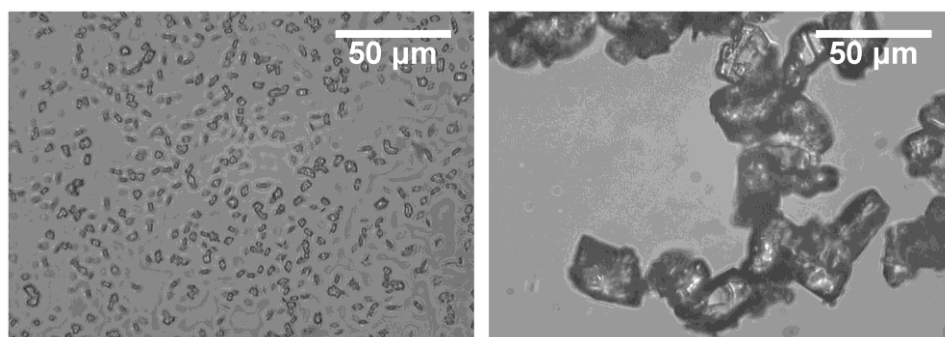
Fig. 3. Different particle sizes in different solvent systems
(left, A: QESD 1, right, B: QESD 2)

In the next step, different types and amounts of emulsifiers were applied to examine their effects on product yield and mean particle size (Table 2.). For these experiments the solvent used was a W/MeOH = 1:3 mixture, the antisolvent was n-heptane and the bridging liquid was MeOH. It was found that the suitable emulsifier was a mixture of the two w/o emulsifiers, Span 80 and Span 20. Increasing the amount of the emulsifier decreased the yield. Adding one drop (20 μl) of emulsifier into a system with a total volume of 15 ml was found to generate the maximum yield.

However, the drops became more stable with the use of suitable emulsifiers, crystals did not agglomerate inside the droplets, resulting in a product with small particle size.

Table 2. Effects of different types and amounts of emulsifiers on product yield and mean particle size

Emulsifier (HLB=7.3)	Emulsifier (µl)	Yield (%)	Methanol (ml)	Water (ml)	n-heptane (ml)	Mean particle size (µm)
–	–	48.2	2.25	0.75	12	20
Span 80/Tween 20	20	14.5	2.25	0.75	12	7
Span 80/Tween 20	40	–	2.25	0.75	12	–
Span 80/Tween 20	100	–	2.25	0.75	12	–
Span 80/Tween 20	200	–	2.25	0.75	12	–
Span 80/Span 20	20	88.0	2.25	0.75	12	6
Span 80/Span 20	40	76.3	2.25	0.75	12	12
Span 80/Span 20	100	74.0	2.25	0.75	12	9
Span 80/Span 20	200	59.4	2.25	0.75	12	12

6.4. Spherical crystallization utilizing non-typical methods

6.4.1. SA method

After the above-mentioned crystallization process ended in 24 hours, constant and long-lasting post-mixing was applied to see whether it can improve particle roundness and aspect ratio or not. This post-crystallization agitation was found to decrease particle size (which was significant after 5 hours of mixing) and neither roundness nor the aspect ratio was modified positively. Changing the good solvent/antisolvent ratio induced differences in crystal size. A DMSO/ethyl acetate system was used in a total volume of 20 ml in ratios of 1:2 (SA 12); 1:5 (SA 15) and 1:10 (SA 110). The solvent/antisolvent ratio of 1:5 was found to produce the largest mean particle size (SA 2: 865 µm), although all of the products were found to have an increased particle size (SA 1: 618 µm, SA 3: 140 µm) compared to the raw material (13 µm). Roundness and aspect ratio values also improved (from 2.37 and 1.67 to 1.85 and 1.46, respectively). Light microscopic images of the products are shown in Fig. 4.
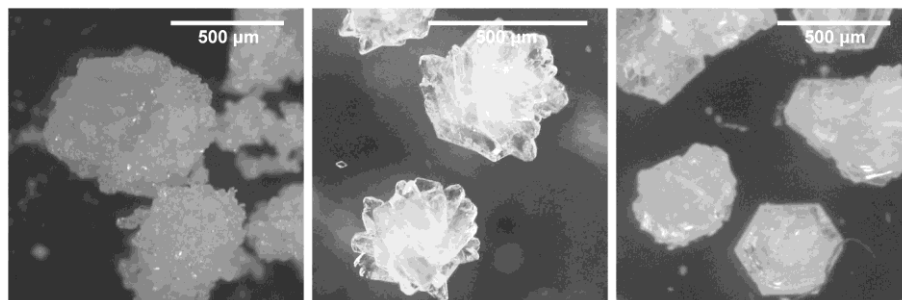
Fig. 4. Crystals produced by the spherical agglomeration method using various ratios of a DMSO/ethyl acetate system (left to right: SA 12, SA 15, SA 110)

The light microscopic images also revealed that these large and nearly-spherical crystals produced by the SA method are not individual crystals but crystal agglomerates.

6.4.2. ATP method

The basis of this method is an alternating temperature profile which includes heating and cooling sections with a permanent heating and cooling rate. Seeding was carried out at 45 °C with the amount of 20 mg seeding crystals of the initial material. For this method two types of mixers were used, a marine propeller and a horizontal shaker. For the different mixers, different crystal morphologies were obtained as shown in Fig. 5.
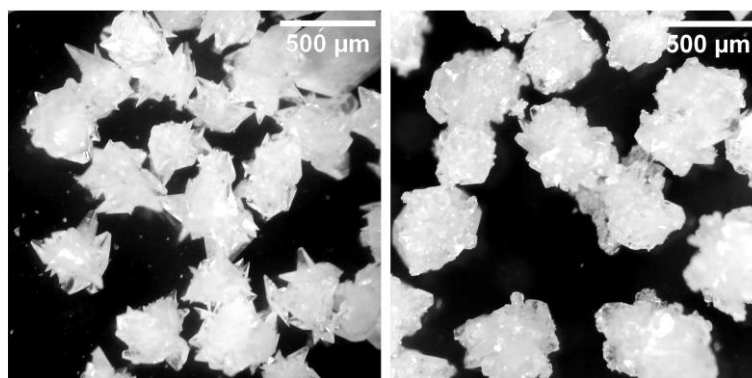
Fig. 5. Effect of different mixer types on crystal habit (marine propeller, left: ATP 2; horizontal shaker, right: ATP 1)

Using the horizontal shaker resulted in larger crystals with a smoother surface (ATP 1) while using the marine propeller resulted in crystals with a spiny surface (ATP 2). In both cases size enlargement (from 13 µm to 260 (ATP 2) and 295 µm

(ATP 1)) and improvement in roundness (from 2.37 to 1.92) and aspect ratio (from 1.67 to 1.64 (ATP 2) and 1.38 (ATP 1)) were observed.

6.5.   Scanning electron microscopy

Scanning electron microscopy analysis was carried out for a detailed characterization of the surface of those particles that had shown significant surface differences in light microscopic images. The spiny particles (ATP 2) were revealed to have a porous structure (Fig. 6.) that may include an increased residual solvent content. In contrast, the particles crystallized in a horizontal shaker had a smooth surface which promotes flowability.
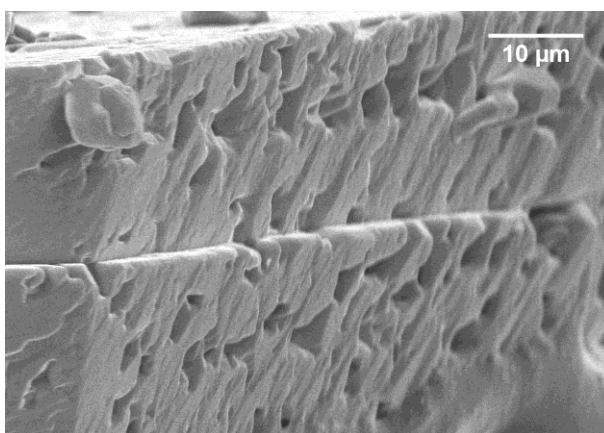
Fig. 6. Porous structure of the spiny particles produced with a marine propeller (ATP 2)

6.6.   Particle size distribution

Particle size distribution was determined by the image analyzer software. The results are shown in Fig. 7.
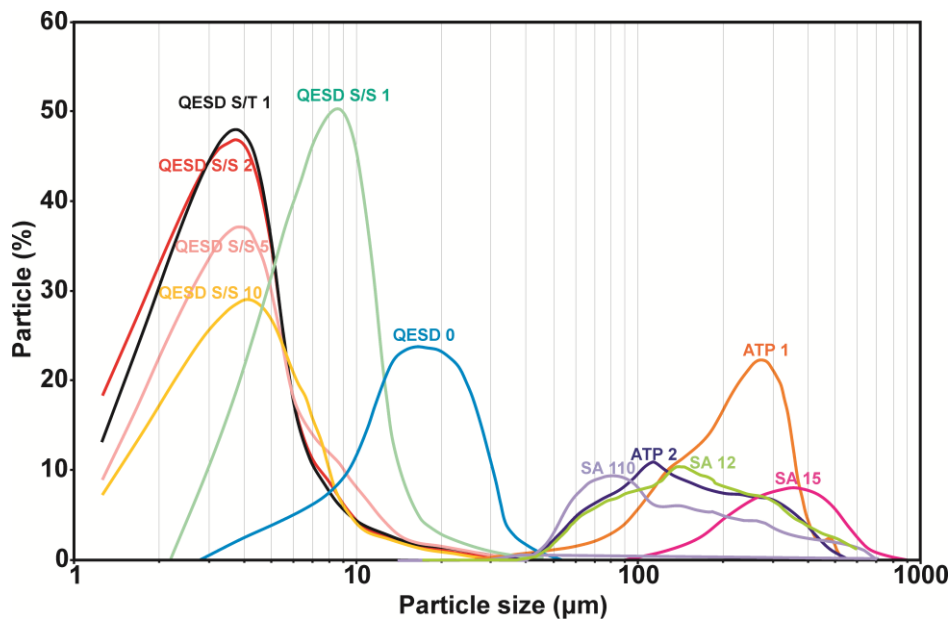
Fig. 7. Particle size distribution of the products (QESD 0: quasi emulsion solvent diffusion method without emulsifier; QESD S/T 1: with 20 µl of Span 80/Tween 20 emulsifier mixture; QESD S/S 1, 2, 5, 10: with 20, 40, 100 and 200 µl of Span 80/Span 20 emulsifier mixture; SA 12, 15, 110: spherical agglomeration with solvent/antisolvent ratios 1:2, 1:5 and 1:10, respectively and ATP 1, 2: cooling crystallization with horizontal shaker and marine propeller agitator, respectively.)

On axis Y, the percentage value is the number of the crystals in the given size range (average width-length, axis X) divided by the number of all particles. The size distributions are monodisperse in case of the QESD products. The ATP and SA methods resulted in wider particle size ranges. It is evident that applying the QESD technique with different amounts of Span 80/Span 20 (S/S) and Span 80/Tween 20 (S/T) emulsifiers (QESD S/S 1, 2, 5, 10 and QESD S/T 1, respectively) results in a small particle size. Without the emulsifiers (QESD 0), the particle size is larger. The non-typical crystallization methods, i.e. ATP 1, 2 and SA 12, 15, 110 yielded larger particles, with SA 15 to produce the largest increase in particle size.

6.7. Polymorphism of the different products

To check if there were any polymorphic transitions during the crystallization procedures, XRPD measurements were carried out. As it is observable in the diffractograms (Fig. 8.), peaks of the crystals produced by the different spherical crystallization techniques and those of the original sample appear at the same 2θ values, indicating that the same polymorphic form was obtained in each case. The

22

observed differences in the relative peak intensities can be attributed to different crystal orientations.
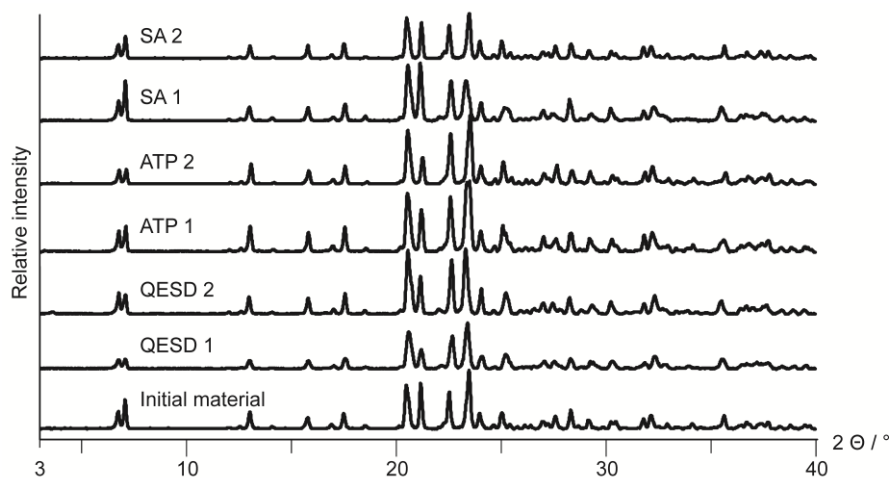
Fig. 8. XRPD diffractograms of the spherical crystallization products

DSC measurements were also carried out since this method, in combination with XRPD, is also a useful tool to clarify if there are any polymorphic transitions. The DSC curves are identical around the melting point, which is between 246 and 247 °C (Fig. 9., left), indicating that all the solid materials are of the same polymorphic form. Exothermic peaks after the melting point refer to decomposition, due to the mass decrease which can be seen in TG curves of Figure 9. (right) around 260°C.
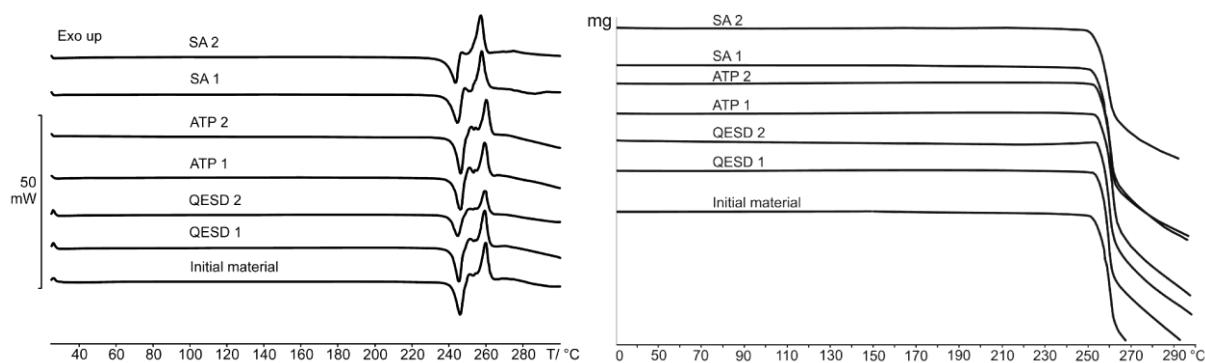
Fig. 9. DSC (left) and TG curves (right) of the AMB HCl crystals produced by different spherical crystallization methods

6.8.   Powder rheology tests

The comparison was carried out between the powder rheological characteristics of the initial material and those of the product (SA 15) with the best mean particle size, aspect ratio, and roundness values. Measurements were executed with the manual method (glass funnel) and with the Pharma Test apparatus (Teflon funnel) and the Stampfvolumeter Stav 2003. The results are summarized in Table 3.

Table 3. Comparison of the powder rheology attributes of the initial material and the product made by spherical agglomeration method

| | **Flow properties** | | | | |
	Flow time (s)		Angle of repose (°)		Characterisation based on *Carr et. al[12]*
Funnel type	glass funnel	Teflon funnel	glass funnel	Teflon funnel	
Initial material	∞	∞	unmeasurable	unmeasurable	**Poor**
SA 15 product	10.72	10.38	34.08	31.4	**Good**
	Compressibility				
	Bulk density (g/ml)	Tapped density (g/ml)	Carr index	Hausner factor	Characterisation based on *Carr et. al[12]*
	Stampfvolumeter				
Initial material	0.54	0.81	32.7	1.49	**Very poor**
SA 15 product	0.50	0.63	20.7	1.26	**Fair/Passable**

Bulk density did not change much, considering, that particle size enlargement has happened during the production of SA 15. Even if the surface of the particles became smoother, which is proved by the microscopic exposure, the density could not change significantly. The initial material has got poor flowing properties, so its flow time could not be measured. Values of the angle of repose show that flowing properties have been improved. Based on the categorization of Carr *et al.*[12], flow property parameters of the SA 15 product are "good" instead of the "poor" categorization of the initial material. Carr index and Hausner factor have improved, too.

6.9.   Mechanical strength test

The fracture curves of twenty SA 15 particles were described by the curve shown in Fig. 10. The typical fracture strength was almost 3 N which shows that the particles

are mechanically stable and hard enough to keep the spherical morphology during different manipulations with the powder.
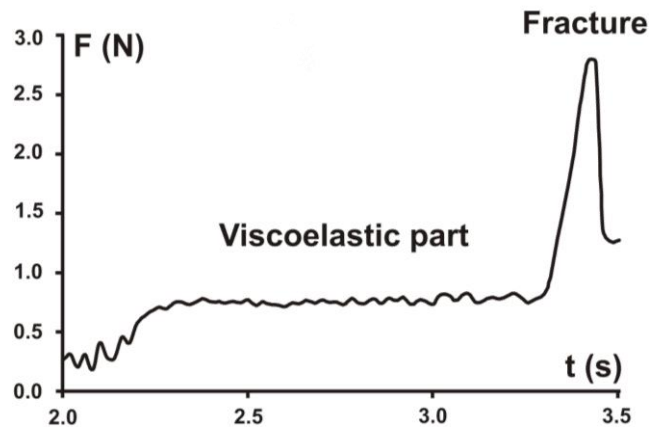

Fig. 10. Typical fracture curve of the SA 15 product

7. Conclusion of the comparison of spherical crystallization methods

Spherical crystals were produced in order to investigate their powder rheology properties for direct compression tablet making and, in the course of our further work, to produce smaller-sized tablets of them.[88]

The solubility of AMB HCl was measured in order to select the proper solvents and antisolvents for each spherical crystallization method. It was investigated as a function of temperature. It was determined in different types of solvents and solvent mixtures. The co-solvent effect of alcohols was found to be significant in each case.

Metastable zone as a function of temperature was determined with an FBRM probe. The MSZW was found to be large which is favorable for cooling crystallization but is disadvantageous for the typical method of spherical crystallization. We have demonstrated that QESD method is suitable for changing the crystal habit. Large-size spherical crystals did not form because of the wide metastable zone, so the diffusion of the alcohol out of the emulsion droplets could not induce enough decrement in saturation rate required for crystal formation. However, the different solvent systems had significant effects on average crystal size. Even when crystallization did occur inside the droplets, particles could not agglomerate.

For AMB HCl, non-typical methods of crystallization like SA and ATP were found to be efficient in terms of increasing particle size and improving roundness. The average size of the particles increased by over an order of magnitude and is now between 80 and 1000 μm which complies with our requirements. Aspect ratio and roundness values are also got closer to the value, 1.00. Different agitation types affected crystal habit variously (Table 4.). SA is the "easiest" method with good yield, causing sightful changes in morphology. The SA 15 product was further investigated by powder rheology and mechanical strength tests, which showed highly improved flowing attributes. Fracture strength of the particles was around 3 N.

Table 4. Critical parameters of the products of different crystallization methods compared to the starting raw material

Method type	Starting material	Typical	Non-typical		
Method name	–	QESD	ATP		SA
Agitator type	–	magnetic stirrer	marine propeller	horizontal shaker	gentle shaking
Roundness	2.37	2.15	1.92	1.92	1.85
Aspect ratio	1.67	1.55	1.64	1.38	1.46
Mean particle size (μm)	13	20	295	260	865

XRPD and DSC studies show no polymorphic transitions for the crystals obtained by the different crystallization methods.

8. Results and discussion 2 – Optimizing the parameters of the SA method

8.1. Risk assessment

8.1.1. Ishikawa diagram

Since the small-volume experiments were promising regarding the SA method, parameter optimization was carried out in order to reveal the design space and improve the morphology. Firstly, an Ishikawa (fishbone) diagram was constructed to identify the effects of key material attributes and process parameters on the development of the production of AMB HCl spherical agglomerates with the SA method (Fig. 11.)
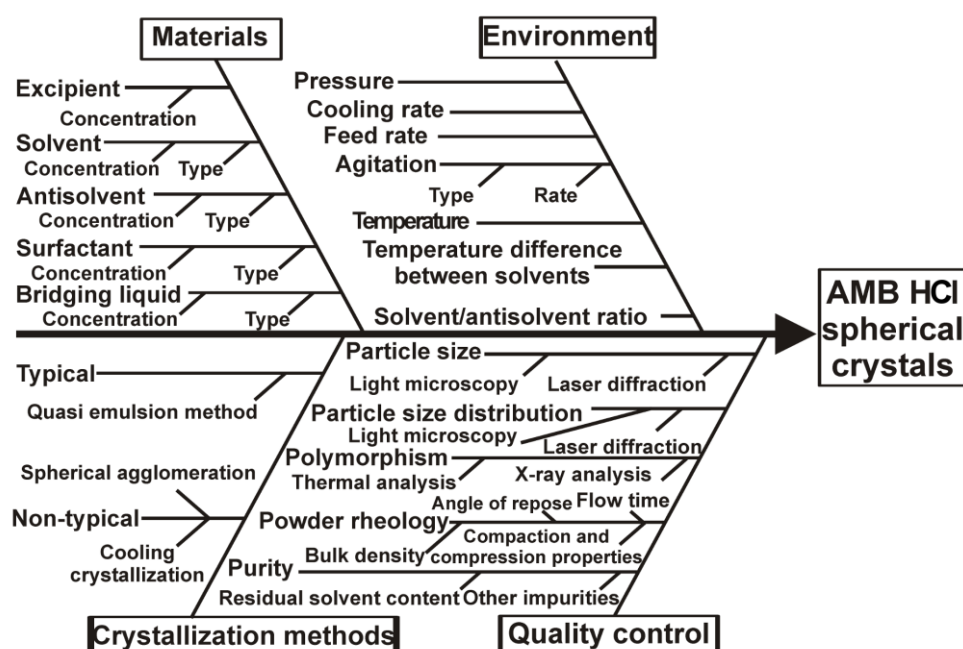
Fig. 11. Isikawa-diagram for the identification of the key parameters for the production of spherical AMB HCl agglomerates

8.1.2. Definition of the QTPPs and identification of the CQAs

On the basis of literature data and pilot experiments, QTTPs and CQAs were determined and are shown in Tables 5-6. together with their justification.

Table 5. QTPPs of the spherical AMB HCl produced by the SA method

QTPP	Target	Justification
Direct compressible crystalline material	Direct compressible	The dosage form of this API is most commonly the tablet. Direct compression tablet making is a simple and fast method and well-usable for active ingredients that are moisture sensitive.[7]
Morphology	Larger, spherical particles.	Larger, spherical particles possess better powder rheology parameters, which simplifies direct tablet making. Direct compression is an easy tableting method which avoids the long process of granulation.[101]
Residual solvent content	The lowest possible, according to ICH guideline Q3C.[102]	Residual solvent content is a critical parameter because its toxic effect on the human body if its amount is higher than a certain described dose.
Habit	Spherical	Spherical crystals can easily roll on each other which predestinate better flowing properties.
Powder rheology attributes	Good flowing properties	Better flowing properties simplify industrial operability of the powder.[103]
Dosage form	Tablet	Tablet is the most common dosage form of this API.[104, 105]
Route of administration	Per oral, GI tract	Ambroxol hydrochloride is most commonly used as a tablet for per oral application.[106]
Therapeutic effect	Expectoration improver	AMB HCl is a clinically proven systemically active mucolytic agent. When administered orally onset of action occurs after about 30 minutes.[107]

Table 6. CQAs of the spherical crystal containing AMB HCl

Quality attributes	Target	Is it a CQA?	Justification
Physical attributes (colour, odour, appearance)	White, odourless powder	No	Physical attributes are not directly related to the patient safety, thus, it is not a critical attribute.
Particle size	Size range: 80-1000 µm	Yes	Particles of this size range are better-applicable for direct compression in case of a high-dose active agent, since adherence and aggregation of the particles are uncharacteristic [108].
Particle size distribution	Narrow size distribution	Yes	Low span values indicate narrow particle size distribution, which makes the powder easy to process.[108]
Roundness	→ 1.00	Yes	This parameter is the measure of how closely the shape of an object approaches that of a mathematically perfect circle. Roundness applies in two dimensions, but it can refer to its three-dimensional analogue, sphericity, as the image analyser software works in 2D, this way spheres are treated as circles.
Aspect ratio	→ 1.00	Yes	This parameter complements roundness very well. If these two are close to 1.00, it means, that the investigated object is close to a sphere or circle.
Angle of repose	25-40° [12]	Yes	These parameters show the powder rheology attributes of the powder. Particles with "good" flowing properties are suitable for direct tablet making.
Flow time	0-10 s [12]	Yes	
Carr index	1-25 [12]	Yes	
Hausner factor	1.00-1.34 [12]	Yes	

After the identification of the QTPPs and the CQAs, the following step is to determine the critical material attributes and process parameters (CMAs and CPPs) by risk estimation matrix (REM), which represents the potential risks associated with each material attribute and process parameter that have a potential effect on CQAs. By assigning a low (L), medium (M) and high (H) values to each parameter, the REM of interdependence rating between the CQAs and QTTPs was established. For the probability rating, a 1(L)-3(M)-9(H) scale was used. The interdependences of the factors are shown in Fig. 12.

QTPPs	Impact	CQAs	CMAs and CPPs	Occurence
Particle size	High	Physical attributes (colour, odour, appearance)	Mixing time (CPP)	High
Morphology	High	Particle size	Mixing type (CPP)	High
Residual solvent cont.	Medium	Particle size distribution	Mixing rate (CPP)	Low
Habit	High	Roundness	Solvent type (CMA)	Medium
Powder rheology attributes	Medium	Aspect ratio	Antisolvent type (CMA)	Medium
Dosage form	Medium	Angle of repose	Solvent/antisolvent ratio (CPP)	Medium
Route of administration	Low	Flow time	dT(between solvent and antisolvent) (CPP)	High
Therapeutic effect	Low	Carr index	Saturation (CPP)	Medium
		Hausner ratio	Feed rate (CPP)	Low

(A): CQA/ QTTP	Direct compressible crystalline material (H)	Morphology (H)	Residual solvent content (M)	Habit (H)	Powder rheology attributes (M)	Dosage form (M)	Route of administ ratoion (L)	Therapeutic effect (L)
Particle size 14%	H	M	M	H	H	L	L	L
Physical attributes 2%	L	L	L	L	L	L	L	L
Size distribution 6%	M	L	L	M	H	L	L	L
Roundness 17%	H	H	L	H	H	L	L	L
Aspect ratio 17%	H	H	L	H	H	L	L	L
Angle of repose 11%	H	M	L	M	H	L	L	L
Flow time 11%	H	M	L	M	H	L	L	L
Carr index 11%	H	M	L	M	H	L	L	L
Hausner factor11%	H	M	L	M	H	L	L	L

(B): CQA/ CPP/CMA	Solvent type	Antisolvent type	Solvent/anti solvent ratio	Saturation	Mixing time	Mixing type	Mixing rate	dT	Feed rate
Particle size 14%	M	M	H	M	H	H	M	H	M
Physical attributes 2%	L	L	L	L	L	L	L	L	L
Size distribution 6%	M	M	M	L	H	H	L	M	M
Roundness 17%	M	M	H	M	H	H	L	H	M
Aspect ratio 17%	M	M	H	M	H	H	L	H	M
Angle of repose 11%	M	M	M	M	H	H	M	H	M
Flow time 11%	M	M	M	M	H	H	M	H	M
Carr index 11%	M	M	M	M	H	H	L	H	M
Hausner factor 11%	M	M	M	M	H	H	L	H	M

Fig. 12. Selected QTPPs, CMAs, CPPs and CQAs and impact on the crystallization system. Selected QTPPs, CMAs, CPPs and CQAs and their interdependence rating with risk estimation matrix (REM): L = low risk parameter; M = medium risk parameter; H= high risk parameter. (A: interdependence between CQAs and QTPPs; B: interdependence between CQAs, CMAs and CPPs)

8.1.3. Pareto analysis

Based on the REM results, a Pareto chart (Fig. 13.) was generated showing the severity scores of CMAs and CPPs. Mixing time and type, dT (temperature difference between solvent and antisolvent) and composition (solvent/antisolvent ratio) were the factors with the highest severity scores (above 9000). During the following experiments, these factors were the independent variables of the factorial design. The Pareto analysis of CQAs led us to the following conclusions: roundness, aspect ratio, and average particle size were the factors with the highest severity scores (above 200), and, according to this, these were the dependent variables of the factorial design in the next step.
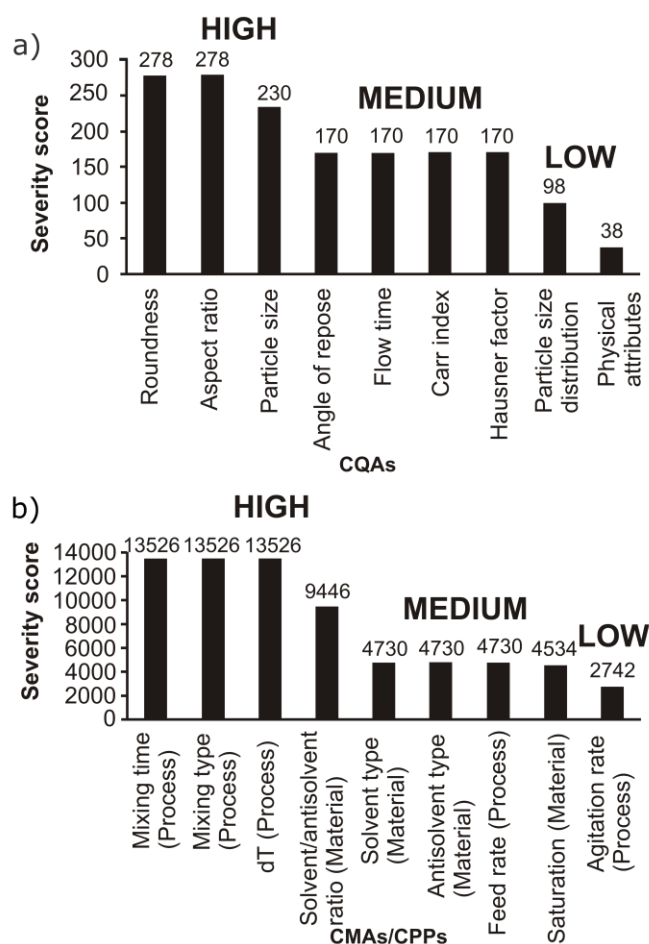
Fig. 13. Pareto-diagrams of the CQAs (a) and the CMAs/ CPPs (b).
Low = low risk parameter; Medium = medium risk parameter; High = high risk parameter.

8.1.4. Factorial design and crystallization

A mixed 2-3-level factorial design was planned considering the critical parameters of the spherical crystals, which were determined by small-volume pre-experiments and evaluated by LeanQbD™ Software: mixing type (qualitative factor), mixing time, dT, composition. They functioned as independent variables. Dependent variables of the factorial design were roundness, aspect ratio and average particle size on the basis of the severity scores of the CQAs. The levels of the factors are shown in Table 7.

Table 7. The levels of the applied factors during the factorial design

Factor	Levels			Number of levels
	Low	Center	High	
Mixing type (qualitative)	horizontal shaker/marine propeller			2
Composition (solvent/antisolvent ratio)	1:5	–	1:10	2
dT (°C)	0	10	20	3
Mixing time (min)	30	90	150	3

For the factorial design, it was necessary to make 36 products for the examination of the variables which were as follows: average size, aspect ratio, roundness, and yield. Each crystallization was carried out three times in order to investigate the reproducibility and relative standard deviation values were calculated, which showed, that the methods were well-reproducible. With the application of STATISTICA 13 for Windows software, significant factors were determined and summarized in Table 8. Reproducibility was also confirmed with 3 parallel measurements. The polynomial functions of the correlations are described, too. In that case, several linear and quadratic factors were neglected in order to improve adjusted R^2, however, decreasing the number of the factors led to the decrement of R^2.

Table 8. Parameters and effects causing significant changes in the dependent variables of the factorial design, applied for the SA method, polynomial functions describing the conditions of significance

Dependent variable	Polynomial function	R^2	Adjusted R^2
Average size	$y=53.97-33.75x_1-\underline{23.60x_2}-\underline{26.09x_3}-14.19x_4+17.39x_4^2+\underline{26.83x_1x_2}+\underline{30.32x_1x_3}+17.35x_1x_4-15.20x_1x_4^2+\underline{31.13x_2x_3}+14.95x_2x_4-\underline{24.79x_2x_4^2}-23.68x_3x_4^2$	0.74	0.58
Aspect ratio	$y=1.508-0.032x_1+\underline{0.032x_2}+0.013x_3^2+0.013x_4^2-0.021x_1x_2-\underline{0.040x_1x_3}-0.016x_1x_3^2-0.021x_2x_4+\underline{0.029x_1x_4}^2+0.021x_3x_4^2+0.018x_3^2x_4+0.022x_3^2x_4^2$	0.61	0.41
Roundness	$y=1.9681-0.013x_1+0.119x_2-0.035x_3-0.011x_4^2-\underline{0.228x_1x_3}+0.095x_2x_3^2$	0.38	0.25
Yield	$y=38.94-0.19x_1+1.46x_2+\underline{9.25x_3}+0.12x_4+\underline{5.66x_3^2}-1.50x_4^2-3.90x_1x_2-\underline{10.47x_1x_3}-3.33x_1x_4-3.56x_1x_4^2-6.92x_2x_3$	0.65	0.49
x_1: Mixing type; x_2: Composition; x_3: Mixing time; x_4: dT			

For more information on the parameters that characterize our design space, surface plot diagrams were also taken (Figure 14.). Figure 14. a) shows the effects of changing the mixing time and the solvent/antisolvent ratio on average size. DS is where lower mixing time values and composition ratios meet. This is true for Figures 14. b) and c), too. The application of lower mixing time and solvent/antisolvent values results in particles with lower aspect ratio and roundness values.
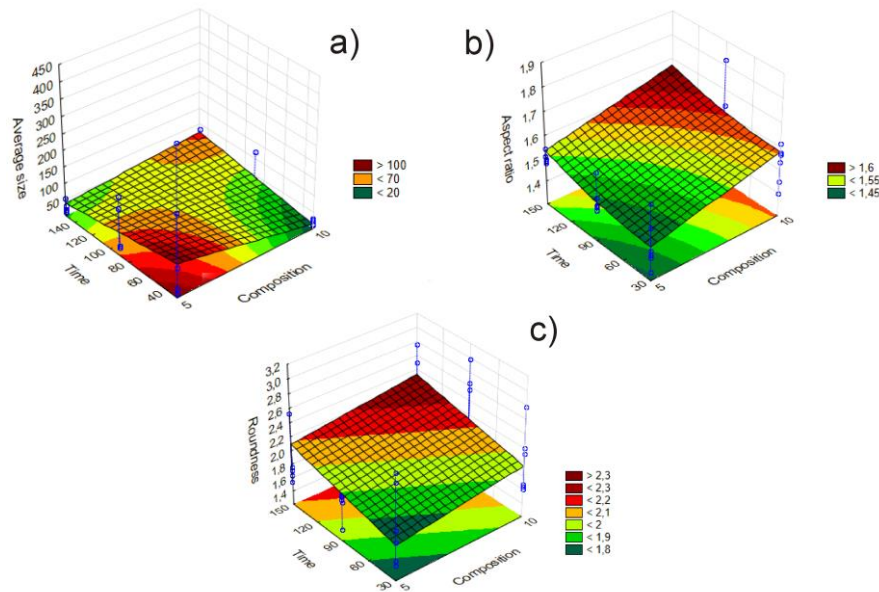

Fig. 14. Surface plot diagrams of the SA products, investigating the effect of mixing time and solvent/antisolvent ratio on average size, aspect ratio and roundness; describing DS

8.2. Light microscopic investigations

During the statistical evaluation of the factorial design of the products, it became clear that four of them (A, B, C, D) have proper average size, aspect ratio, and

roundness values compared to the target product. Average size and roundness values were determined by light microscopic analysis. These values are shown in Table 9.

Table 9. Comparison of the initial material and the products made by spherical agglomeration method (L = low risk parameter; M = medium risk parameter; H = high risk parameter)

	Initial material	A	B	C	D
Average size (μm)	13.12	248.17	176.82	142.50	441.53
Aspect ratio	1.67	1.34	1.43	1.45	1.40
Roundness	2.37	1.41	1.37	1.88	1.49
Yield (%)	-	37.46	32.17	14.14	18.98
Applied parameters					
Mixing type	-	Horizontal shaker			
Composition	-	1:5			
Mixing time (min)	-	90 (M)	30 (L)	90 (M)	30 (L)
dT	-	0 (L)	0 (L)	10 (M)	10 (M)

Compared to the initial material, over an order of magnitude increase was reached and both aspect ratio and roundness values improved. Light microscopic images were taken in order to observe the morphology of the particles more closely. Exposures of the initial material and products A, B, C, and D are shown in Figure 15.
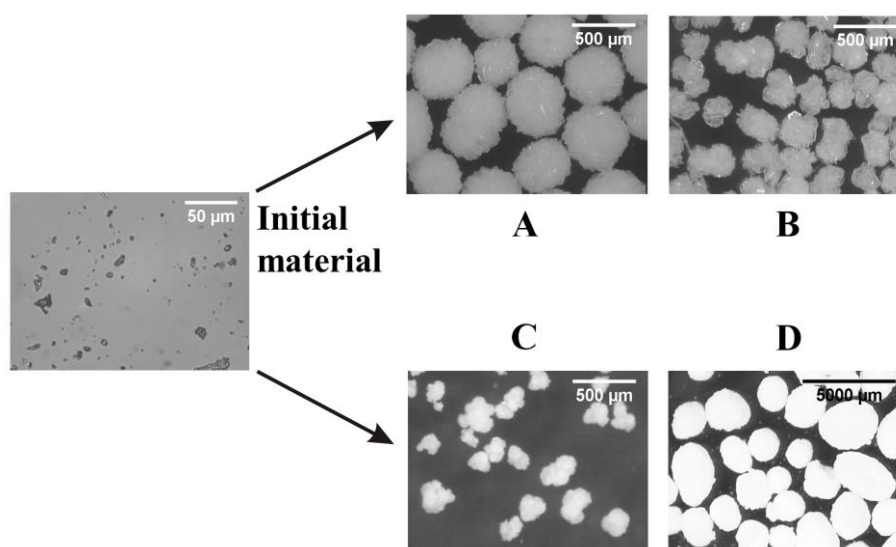

Fig. 15. Light microscopic measurements of the initial material and the SA products produced with the application of different process parameters

These measurements confirmed that roundness values improved and the surface of the crystals became generally smoother (Figure 15. A, B, C, D). On the basis of the

light microscopic images, the SA method also enabled the production of uniform crystals.

8.3. Polymorphism of the SA products

After crystallization, it was necessary to verify that no polymorphic transitions happened. For this, XRPD and DSC were used, and it can be claimed that the crystalline material is of the same polymorphic form during the crystallization procedure (Fig. 16.). It can also be compared with the former investigations of polymorphy and it can be said, that the DSC and XRPD curves are the same that those of the initial material.
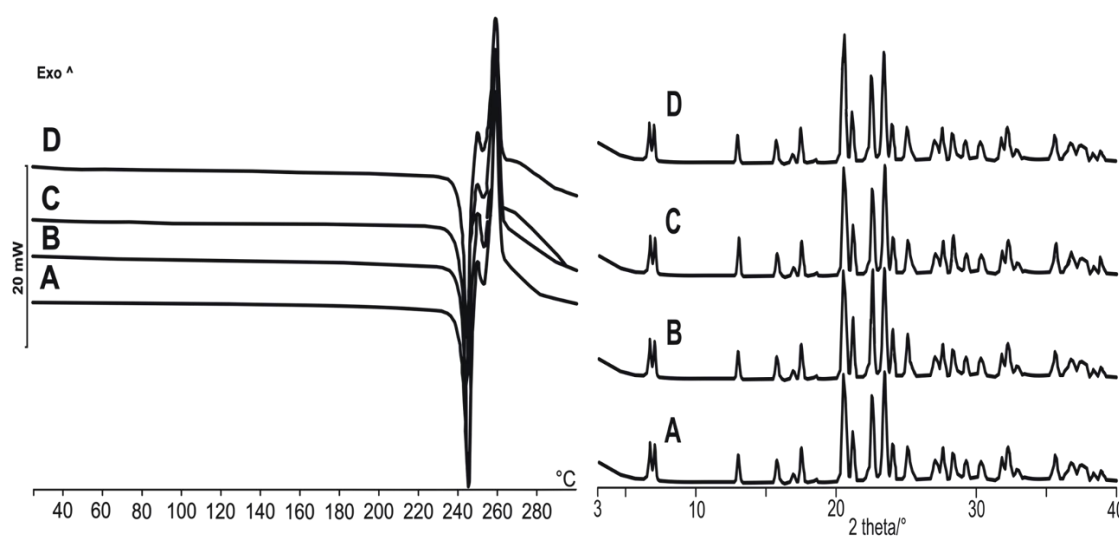
Fig. 16. XRPD and DSC results of the four products with proper average size, aspect ratio and roundness values (SA/ A, B, C, D products)

8.4. Powder rheology tests

Product B was chosen for this experiment because the highest amount could be produced of this one (short mixing time, dT = 0 °C). Powder rheological properties were investigated and it was revealed that product A had far better flowing properties. The Carr index and the Hausner ratio also showed improvements compared to the initial material. This can facilitate the tableting process (for example, direct compression can be used instead of conventional tableting methods) and any other manipulations during the production (e.g. loading). Therefore, in the case of direct compression tablet making, the amount of the additives may be

reduced. In Table 10. improvements in powder rheological properties are summarized.

Table 10. Improvements in powder rheological properties comparing the initial material and the SA (B) product

	Bulk density (g/ml)	Tapped density (g/ml)	Flow time (s)	Angle of repose (°)	Carr index	Hausner factor	Classification (*Carr et al* [12].)
Initial AMB HCl	0.54	0.81	unmeasurable	unmeasurable	32.67	1.49	Very poor
SA product	0.43	0.53	13.6	31.3	18.8	1.23	Fair

8.5. Mechanical strength test

Mechanical strength tests were carried out in order to examine the mechanical stability of the crystalline material. The fracture curves of the products showed enough mechanical strength to maintain their spherical morphology with 2.53-3.13 N of fracture forces (Table 11.), which is a specifically high value regarding the average size of the particles.

Table 11. Mean values of the fracture forces of SA products based on 20 measurements

Sample	Fracture force (N)
A	2.95 ± 0.06
B	3.02 ± 0.04
C	2.53 ± 0.07
D	3.13 ± 0.04

The fracture curves of products SA/ A, B, C and D are shown in Figure 17.
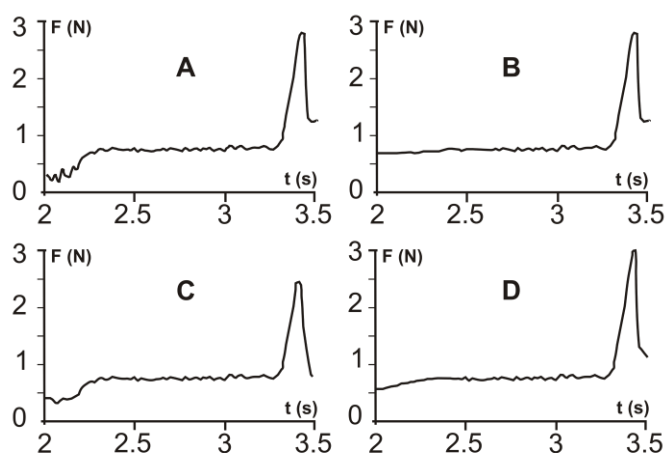

Fig. 17. Representative fracture curves of the spherical agglomerates produced by the SA method

With a relatively long viscoelastic period, it can be claimed, that the particles are resistant to slight mechanical impacts and only a relatively large force could break the particles, which is advantageous throughout the handling of the crystalline material during the production.

9. Conclusion of the process optimization by means of Quality by Design approach

The SA method was applied on the active agent, AMB HCl in order to improve its powder rheological properties, which can ease the application of direct compression tablet making. The crystallization method was preceded by risk assessment. The QTPPs, CQAs, CMAs and CPPs were determined and risk severity scores were evaluated by the Lean QbD program. According to the results, independent and dependent variables for a mixed 2-3 factorial design were determined and the factorial design was established. A total of 36 products were prepared. Four of them (A, B, C, D) were marked as „good" for further investigations. Firstly, during the product assay, it was verified, that no polymorphic transitions happened throughout the crystallization procedure. For this, X-ray powder diffraction (XRPD) and thermal analysis (DSC) were applied. With light microscopic measurements, average size, roundness, and aspect ratio were determined or calculated and, compared to the initial material, they showed large betterment. Powder rheological properties were also examined. Flow time, the angle of repose, bulk density and tapped density values were measured, and the Carr index and the Hausner factor were calculated and compared to these of the initial material. A large improvement in these parameters was observed, and also the mean particle size became also appropriate for direct compression, which is the topic of our next study. Mechanical strength characteristics were also investigated in order to predict whether the products are suitable for pharmaceutical manipulations like filling, and it was revealed that the particles are stable and hard enough to keep their morphology constant during these procedures. Summarizing the main discoveries of the research, spherical agglomeration crystallization process was applied successfully on the compound, AMB HCl, resulting in spherical particles (140-450 µm) with a smooth surface and improved powder rheological properties. The method was coupled with risk assessment which was applied as a part of process development. It is a fairly

individual and economical way for the production of AMB HCl crystals because it is based on the main impacts and experiments could be built up based on a factorial design, and this way less solid material and solvents were used compared to the original method, which starts with dozens of pre-experiments.

10. Results and discussion 3 - FBRM observation of the non-typical methods, SA and ATP

With the help of FBRM, spherical crystallization of SA/A, B, C, D products was observed. The same was performed in the case of the ATP method. Chord length values were evaluated.

As for the SA 1 method, we can say that the FBRM showed almost the same pattern in both cases, therefore only the experiments carried out under $dT = 0$ °C are shown in Fig. 18, where the change of the total particle number is presented as a function of experiment time.
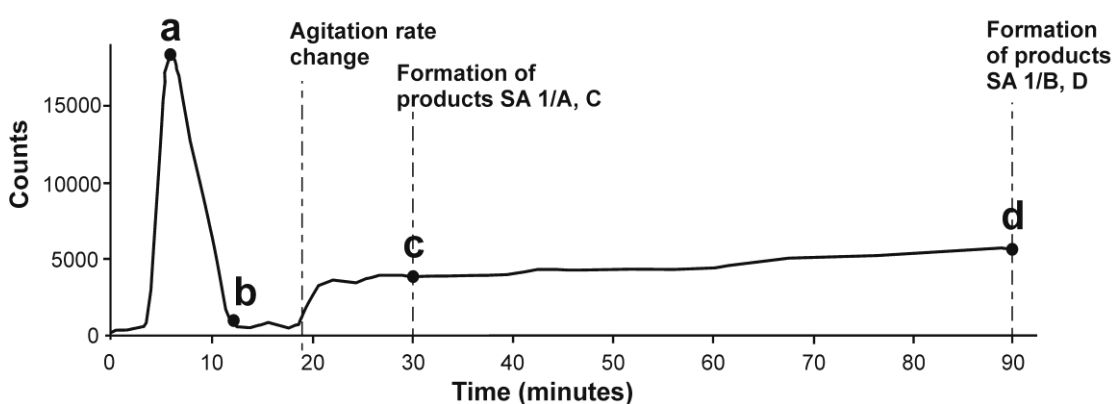

Fig. 18. FBRM curves of the formation mechanism of SA 1/A, B, C, D products

In the point, where the addition of the saturated solution to the antisolvent happened, the particle number started to increase up to ~ 19000 counts (point "a"). A decrease can be observed after 10 minutes of the addition ("b"), which was caused by the sedimentation of the larger, newly-agglomerated particles, so it can refer to the agglomeration itself, as well. Possibly this is due to the low agitation rate (150 rpm), which was insufficient for this crystallization method since it was not able to pick up the larger particles from the bottom of the reactor. About 20 minutes after the addition, a more intense agitation (250 rpm) was applied in order to prevent the high-level sedimentation at the bottom of the reactor. At this point, the particle number increased (up to ~ 5000 counts) as well as the chord length values. In Table 12, chord length values contributed to the points marked with letters are shown. It can be concluded, that after the agitation rate was changed to a higher one, the average chord length increased because the larger, sedentary crystals could also flow at 250 rpm.

SA products (A, B, C, D) were also manufactured in the larger-scale reactor (SA 2 experiment set). The curves for dT = 0 °C and dT = 10 °C experiments looked almost the same, therefore FBRM curves are shown only in the dT = 0 °C case (Fig. 19.).
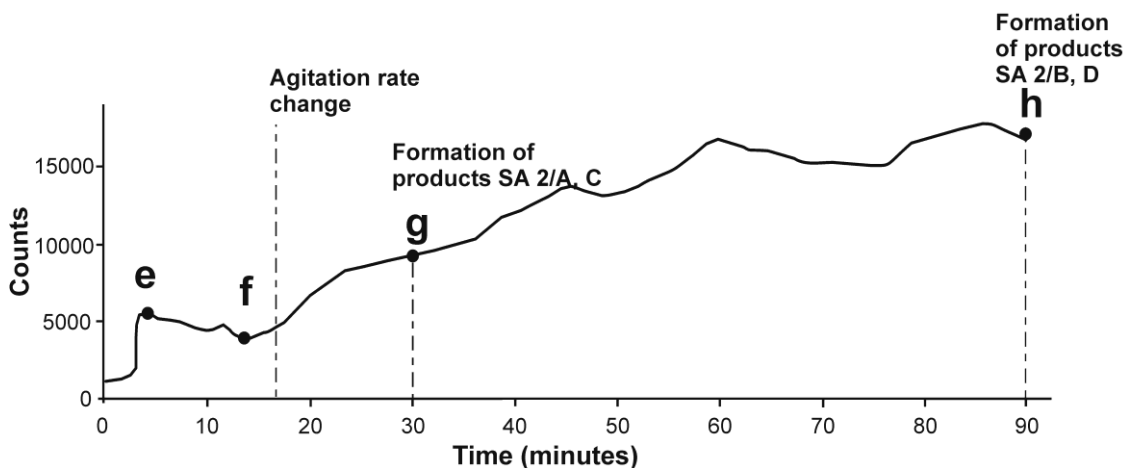
Fig. 19. FBRM curve of the crystallization of SA 2/ A, B, C and D applying the larger-scale reactor

Chord length values are presented in Table 12.

Table 12. Average chord length values of the marked points shown in Fig. 18-19, SA 1 and 2 methods

Point	Chord length (mean square weight, μm)	Point	Chord length (mean square weight, μm)
a	68	e	162
b	134	f	215
c	141	g	243
d	130	h	195

On the basis of the FBRM data, counts increased up to point "e" after the addition of the solvent to the antisolvent and decreased until point "f". At about 20 minutes of agitation with 150 rpm, the agitation rate was increased to 250 rpm in order to let the larger, sedimented particles flow. It can be seen that the number of counts increased after this step. It is also observable in point "f" that a decrease in the number of counts happened. This definitely refers to agglomeration because, in parallel, a large chord length increment appeared. It can be concluded that the first 10 minutes of the

process was critical regarding the formation of agglomerates. It is also remarkable that at this part an almost constant increase of the average chord length values can be observed, which correlates well with our previous results in connection with the parameter optimization of the SA method. It should be emphasized that in points "d" and "h" a slight chord length decrement can be observed due to the intensive and long-term agitation, which can cause the breakage of the particles, especially if they are agglomerations, not individual crystals. This phenomenon is more significant when agitation by the marine propeller was applied. It caused smaller, floating pieces in the system, which lowered the average chord length value. The optimization of the agitation is essential.

The ATP method was applied in the small- (ATP 1) and also in the larger-scale (ATP 2) reactor. The evaluation of the FBRM curve of the ATP 1 method can be seen in Fig. 20.
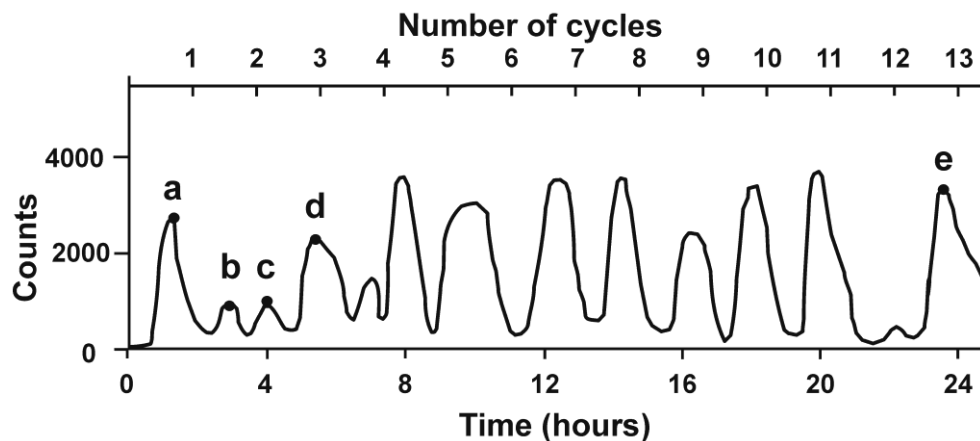
Fig. 20. FBRM curve of the small-scale ATP 1 method applying horizontal shaker

During the first cooling cycle, counts increased as precipitation happened (Table 13). After the second cycle, the mean particle size increased over an order of magnitude. What was not expected was the decrement of the particle size during the third cooling cycle, which is probably due to the sedimentation of the larger particles, that could not be measured and count into the statistics. It can be seen that number of counts decreased in the case of points "b" and "c". The theory is that the agglomeration of the particles happened during this second and third cooling cycle

because the chord length values increased. It can be said that the agitation rate needs to be more intense for this measuring method because in this case turbulent flow was very low and sedimentation could happen easily, even on the probe itself, which can be related to the initial material's predisposition to adhesion.

Table 13. Chord length values of the pinned points shown in Fig. 20-21, ATP 1 and 2 methods

Point	Chord length (mean square weight, μm)	Point	Chord length (mean square weight, μm)
a	28	f	96
b	64	g	125
c	234	h	172
d	186	i	198
e	218	j	207

In the case of the large-scale reactor, FBRM results are shown in Fig. 21. Several heating-cooling cycles were carried out in order to investigate the mechanism of the agglomeration process.
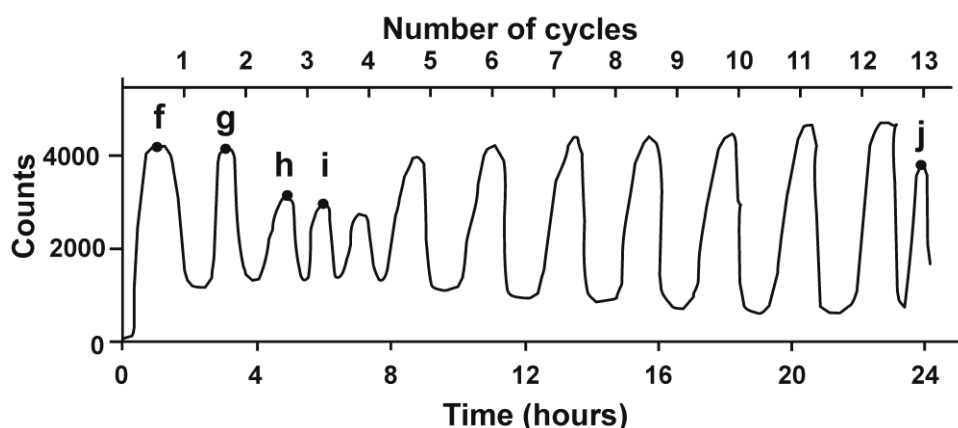
Fig. 21. FBRM curve of the large-scale ATP 2 method applying marine propeller

It can be concluded on the basis of Table 13, that after the first cooling cycle, in point "f", the number of counts increased and the average chord length value is around 96 μm. During the process, constant chord length increment was experienced, which is different from the ATP 1 method, where a significant level of sedimentation took place. The marine propeller could produce a higher level of turbulent flow, which hindered the particles from the adhesion to the glass wall, the thermometer or the probe. In points "h" and "i" we could observe a little decrement in the number of counts and an increase in the chord length values, which could be assigned to the agglomeration of the particles. In the case of the ATP 1 method, it had already

started by the second cooling cycle, but as for the ATP 2 experiment, it started only in the third cycle.

10.1. Comparison of the SA 1-2 and ATP 1-2 methods

Crystallization types were compared in the case of using a double-walled glass reactor of 250 ml with a total solvent volume of 80 ml and, as a scale-up, a jacketed reactor of 750 ml with a total solvent volume of 500 ml, while applying different types of agitation.

The first crystallization type was the SA method. After the small-scale reactor, A, B, C and D products were also prepared in the larger reactor. Particle size differences are shown in Table 14.

Table 14. Comparison of the particle sizes of the crystals produced under different circumstances of the SA method

Initial material		
Aspect ratio	Roundness	Average size (µm)
1.67	2.37	13.12

SA 1-2					
	Small reactor, horizontal shaker (SA 1)			Large reactor, marine propeller (SA 2)	
Sample name	Aspect ratio	Roundness	Average size (µm)	Aspect ratio	Roundness	Average size (µm)
A	1.36	1.48	123	1.30	1.71	178
B	1.36	1.51	125	1.31	1.78	175
C	1.37	1.54	100	1.35	1.74	158
D	1.33	1.50	157	1.30	1.65	136

It can be concluded that a scale-up of one order of magnitude could be achieved, while the aspect ratio values remained nearly the same. Roundness showed somewhat better values in the case of the SA 1 method due to the rolling effect of the horizontal shaker. The average size values seemed to increase when the marine propeller is used, which could be caused by the turbulent flowing. In this case, individual particles were able to agglomerate with each other from both sides, while the horizontal shaker shaped spherical crystals by rolling them at the bottom or the walls of the reactor, which means that one side is always hampered from cohesion to another particle. Although this effect caused lower particle size values, the horizontal

shaker helped to improve the roundness values of the crystals by the constant rolling. Our results achieved with the ATP method, are summarized in Table 15.

Table 15. Comparison of the particle size values of the crystals produced under different scenarios of the ATP method

Initial material		
Aspect ratio	Roundness	Average size (μm)
1.67	2.37	13.12

ATP 1-2					
	Small reactor, horizontal shaker (ATP 1)			Large reactor, marine propeller (ATP 2)		
Cycle number	Aspect ratio	Roundness	Average size (μm)	Aspect ratio	Roundness	Average size (μm)
1st	1.37	1.55	141	1.50	1.64	125
2nd	1.29	1.67	219	1.29	1.46	152
3rd	1.30	1.41	345	1.23	1.52	183
4th	1.30	1.35	395	1.24	1.38	197
13th	1.30	1.32	404	1.27	1.31	298

In the case of ATP methods, samples were taken out after the 1st, 2nd, 3rd, 4th and 13th cooling cycles to describe the level of the improvements in the particle size, aspect ratio and roundness (Table 15). We can see that in the case of ATP 1, because of the agitation type, the agglomeration of the crystals was remarkable. This is why the mean particle size values are larger than those obtained with the ATP 2 method. This correlates with our previous experiences. [88] It can also be concluded that, while the average particle size constantly increased with the number of cycles, roundness seemed to show only a slight improvement and the aspect ratio values stagnated after the 3rd cycle.

10.2. Light microscopic images

Light microscopic images were taken for investigating the surface and size enlargement of the SA products. The exposures are shown in Fig. 22.
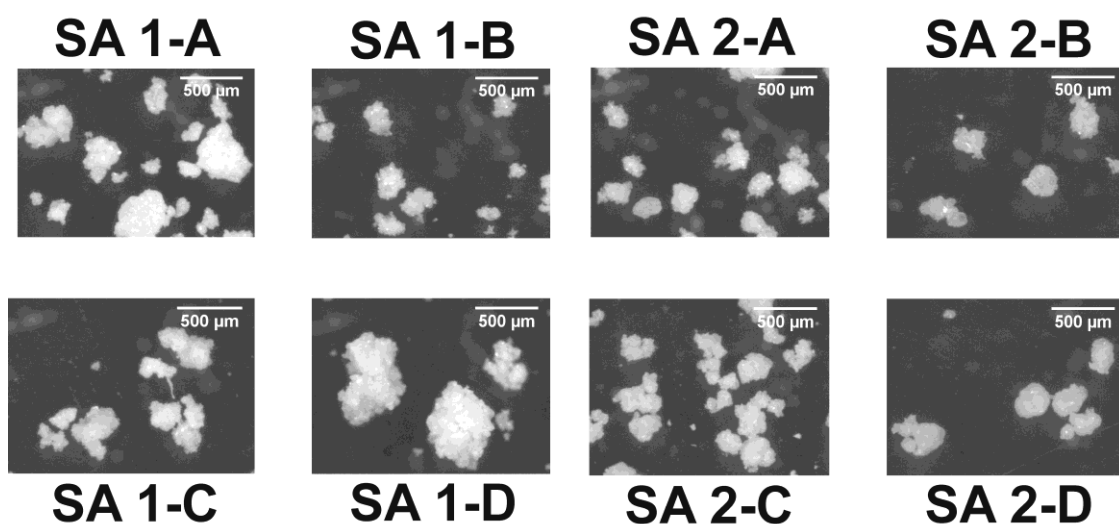
Fig. 22. Surface and size properties based on the light microscopic images of SA 1 and 2 products

It can be observed that the particles mostly form agglomerates in comparison to the ATP 1 and 2 products (below), where the crystal growth is more significant than the agglomeration, therefore individual particles are yielded.

The products of the ATP 1 and 2 methods were compared from the aspect of surface smoothness, morphology, and size. In Fig. 23, the surface changes can be observed in the case of ATP 1 and ATP 2 methods.
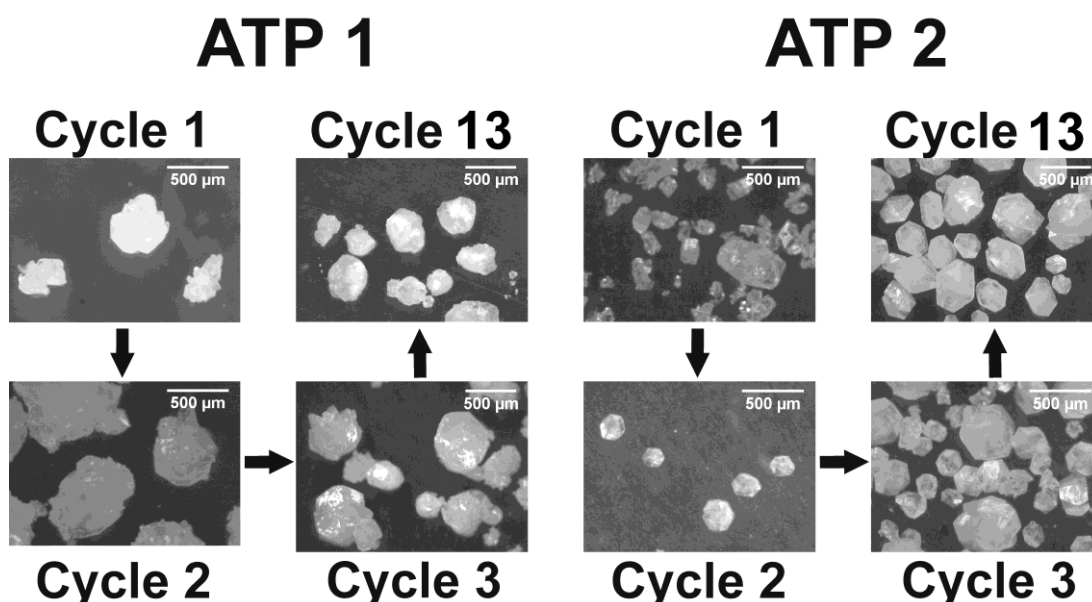
Fig. 23. Surface and size changes based on the light microscopic exposures after the cooling cycles of the ATP 1 and 2 methods

The exposures clearly reveal that a size enlargement happened in both cases. It is also observable that the surface of the particles became smoother after each cooling

cycle. It is remarkable how roundness improved during the second cooling cycle of ATP 2.

10.3. Residual solvent content

Residual solvent content of the optimized products was analyzed and the results are summarized in Table 15.

Table 15. Resuidual solvent contents of the optimized products compared to the ICH Q3C Guideline limits

Sample	MeOH (ppm)	Ethyl acetate (ppm)	DMSO (ppm)
ATP 1	226		
ATP 2	0		
SA 1 - A		735	2038
SA 1 - B		854	4448
SA 1 - C		1124	3167
SA 1 - D		1642	1817
SA 2 - A		2221	1629
SA 2 - B		2233	2826
SA 2 - C		1549	1433
SA 2 - D		1648	1925
Solvent class	2	3	3
ICH Q3 limit (ppm)	<3000	<5000	<5000

It can be concluded that the residual solvent content of the products are under the Class 2 and Class 3 limits which are described in the ICH Q3C Guideline.

11.   Conclusions of the on-line measurements

In the course of the current experiments, SA and ATP crystallization methods were applied and the products were evaluated from the aspects of average particle size, aspect ratio, and roundness. Based on the FBRM results, it was revealed that the marine propeller was a more suitable agitation type than the horizontal shaker because in the case of the marine propeller the particles could flow properly, which could enhance crystal growth since particles were not hindered from either side.

It is also concluded that with the use of the SA method, the critical agglomeration-forming section of the process was within the first 10 minutes from the addition of the solution to the antisolvent. This could be concluded based on the FBRM data, which showed decreasing chord length and count number values, due to the sedimentation of the larger agglomerates.

When ATP methods were used, additional cooling cycles caused a constant improvement in the average size of the particles, but after the second cycle, roundness seemed to show non-significant changes, and aspect ratio values stagnated after the additional cycles.

From the light microscopic exposures, it could be concluded that the ATP 1 and 2 methods seemed to be more suitable for the production of larger, individual particles, while mostly crystal agglomerates were formed with the SA 1-2 methods.

12.   Final conclusions and achievements of the work

This is the first study on the application, optimization, and comparison of typical and non-typical spherical crystallization types applied to the model drug, AMB HCl. It was revealed, that in case of this crystalline material, non-typical crystallization methods were the most suitable ones to produce large-size, well-flowing spherical crystals or crystal agglomerates. These methods (ATP and SA) were further investigated and optimized. The particles with the best average size – aspect ratio and roundness values were characterized by their powder rheological attributes. Flow and compaction properties were determined and calculated (Carr index and Hausner ratio) and these values were also compared those of the initial material. A considerable improvement was achieved compared to the initial material, thus, we can say, that the applied two, non-typical crystallization methods can be used to change the morphology of the crystals in a favorable way. For a proper industrial process development, risk assessment and parameter optimization are indispensable. These two were carried out applying the principles of the Quality by Design approach. After the determination of the QTPPs, CQAs, CMAs, and CPPs, a factorial design was planned and crystals were produced with various process parameters. Among the products, there were four (SA/A, B, C, D) that suited the requirements (80 μm < mean particle size < 1000 μm), which were tested for reproducibility and their features were input in Statistica for Windows and then evaluated. The significant effects were determined. After the SA product, it was necessary to test the ATP method, as well. In this case, there were fewer process parameters, therefore the number of the heating-cooling cycles and the mixing type were considered responsible for most of the morphological changes. We carried out experiments to figure out, during which cycle did the largest change happen and it was revealed, that after the 3rd cycle, there were no significant improvements in aspect ratio and roundness values, however, average size constantly increased. With the use of marine propeller mixer, the breakage of the particles was significant, especially after a longer period of mixing. We also observed the crystal formation mechanisms in the SA methods, with the help of focused beam reflectance measurements. The critical crystal-formation period took place mostly within the first 10 minutes of the crystallization and longer agitation with propeller mixer also caused particle-fracture.

Aware of these pieces of information it can be concluded, that we successfully developed two well-applicable methods for the spherical crystallization of AMB HCl, which – with the improved powder rheological properties – can ease the tablet production and can reduce loss during the process.

Aknowlegdements

I am grateful to my supervisor Dr. habil. Zoltán Aigner Ph.D. present associate professor of the Institute of Pharmaceutical Technology and Regulatory Affairs for his enthusiastic guidance of my work.

I would like to express my warm thanks to Professor Dr. Piroska Szabó-Révész and Dr. habil. Ildikó Csóka ex and current Heads of Institute of Pharmaceutical Technology and Regulatory Affairs for providing me the possibility to start my research in the Institute as a chemist, the encouragement, and support throughout my Ph.D. studies.

I would like to thank Klára Kovács, Eszter Molnár, and Éva Oláh the excellent technical support.

I would also like to express my gratitude to all my co-authors and collaborators for the help either it was measurements with a new apparatus, using a new program or analyzing statistical data.

References

1.	Diao, Y.; Harada, T.; Myerson, A. S.; Hatton, T. A.; Trout, B. L., The role of nanopore shape in surface-induced crystallization. *Nat Mater* **2011,** *10* (11), 867-871.
2.	Tahara, K.; O'Mahony, M.; Myerson, A. S., Continuous Spherical Crystallization of Albuterol Sulfate with Solvent Recycle System. *Cryst Growth Des* **2015,** *15* (10), 5149-5156.
3.	Kawashima, Y.; Imai, A.; Takeuchi, H.; Yamamoto, H.; Kamiya, K.; Hino, T., Improved flowability and compactibility of spherically agglomerated crystals of ascorbic acid for direct tableting designed by spherical crystallization process. *Powder Technol* **2003,** *130* (1-3), 283-289.
4.	Nokhodchi, A.; Maghsoodi, M.; Hassan-Zadeh, D.; Barzegar-Jalali, M., Preparation of agglomerated crystals for improving flowability and compactibility of poorly flowable and compactible drugs and excipients. *Powder Technol* **2007,** *175* (2), 73-81.
5.	Akhgari, A.; Sadeghi, H.; Dabbagh, M. A., Modification of flow and compressibility of corn starch using quasi-emulsion solvent diffusion method. *Iran J Basic Med Sci* **2014,** *17* (8), 553-559.
6.	Trementozzi, A. N.; Leung, C. Y.; Osei-Yeboah, F.; Irdam, E.; Lin, Y. Q.; MacPhee, J. M.; Boulas, P.; Karki, S. B.; Zawaneh, P. N., Engineered particles demonstrate improved flow properties at elevated drug loadings for direct compression manufacturing. *Int J Pharmaceut* **2017,** *523* (1), 133-141.
7.	Hirschberg, C.; Sun, C. C.; Rantanen, J., Analytical method development for powder characterization: Visualization of the critical drug loading affecting the processability of a formulation for direct compression. *J Pharmaceut Biomed* **2016,** *128*, 462-468.
8.	Nakamura, S.; Ishii, N.; Nakashima, N.; Sakamoto, T.; Yuasa, H., Evaluation of Sucrose Fatty Acid Esters as Lubricants in Tablet Manufacturing. *Chem Pharm Bull* **2017,** *65* (5), 432-441.
9.	Urquhart, J., Patient compliance with crucial drug regimens: Implications for prostate cancer. *Eur Urol* **1996,** *29*, 124-131.
10.	Shekunov, B. Y.; York, P., Crystallization processes in pharmaceutical technology and drug delivery design. *J Cryst Growth* **2000,** *211* (1-4), 122-136.
11.	Muller, M.; Schneeberger, R.; Wieckhusen, D.; Cooper, M., Example of finishing technologies as key elements for successful active pharmaceutical ingredient process development. *Org Process Res Dev* **2004,** *8* (3), 376-380.
12.	Carr, R. L., Evaluating flow properties of solids. *Chem Eng* **1965,** *72* 163-8.
13.	Kawashima, Y.; Cui, F.; Takeuchi, H.; Niwa, T.; Hino, T.; Kiuchi, K., Improvements in Flowability and Compressibility of Pharmaceutical Crystals for Direct Tabletting by Spherical Crystallization with a 2-Solvent System. *Powder Technol* **1994,** *78* (2), 151-157.
14.	Chatterjee, A.; Gupta, M. M.; Srivastava, B., Spherical crystallization: A technique use to reform solubility and flow property of active pharmaceutical ingredients. *Int J Pharm Investig* **2017,** *7* (1), 4-9.
15.	Worku, Z. A.; Kumar, D.; Gomes, J. V.; He, Y. L.; Glennon, B.; Ramisetty, K. A.; Rasmuson, A. C.; O'Connell, P.; Gallagher, K. H.; Woods, T.; Shastri, N. R.; Healy, A. M., Modelling and understanding powder flow properties and

compactability of selected active pharmaceutical ingredients, excipients and physical mixtures from critical material properties. *Int J Pharmaceut* **2017,** *531* (1), 191-204.

16. Tari, T.; Fekete, Z.; Szabo-Revesz, P.; Aigner, Z., Reduction of glycine particle size by impinging jet crystallization. *Int J Pharmaceut* **2015,** *478* (1), 96-102.

17. Ambrus, R.; Amirzadi, N. N.; Szabo-Revesz, P., Formulation of poorly water-soluble Gemfibrozil applying power ultrasound. *Ultrason Sonochem* **2012,** *19* (2), 286-291.

18. Maja Šantl, I. I., Franc Vrecer, Sasa Baumgartner, A compressibility and compactibility study of real tableting mixtures: The effect of granule particle size. *Acta Pharmaceut* **2012,** *62*, 325-340.

19. McCormick, D., Evolutions in Direct Compression. *Pharmaceutical Technology* **2005 April,** 52-62. Accessible: www.pharmatech.com, 2018.05.29.

20. Doki, N.; Kubota, N.; Sato, A.; Yokota, M., Effect of cooling mode on product crystal size in seeded batch crystallization of potassium alum. *Chem Eng J* **2001,** *81* (1-3), 313-316.

21. Szabo-Revesz, P.; Hasznos-Nezdei, M.; Farkas, B.; Goczo, H.; Pintye-Hodi, K.; Eros, I., Crystal growth of drug materials by spherical crystallization. *J Cryst Growth* **2002,** *237*, 2240-2245.

22. Szabo-Revesz, P.; Goczo, H.; Pintye-Hodi, K.; Kasa, P.; Eros, I.; Hasznos-Nezdei, M.; Farkas, B., Development of spherical crystal agglomerates of an aspartic acid salt for direct tablet making. *Powder Technol* **2001,** *114* (1-3), 118-124.

23. Goczo, H.; Szabo-Revesz, P.; Farkas, B.; Hasznos-Nezdei, M.; Serwanis, S. F.; Pintye-Hodi, K.; Kasa, P.; Eros, I.; Antal, I.; Marton, S., Development of spherical crystals of acetylsalicylic acid for direct tablet-making. *Chem Pharm Bull* **2000,** *48* (12), 1877-1881.

24. Ettabia, A.; Joiris, E.; GuyotHermann, A. M.; Guyot, J. C., Preparation of a pure paracetamol for direct compression by spherical agglomeration. *Pharm Ind* **1997,** *59* (7), 625-631.

25. Kachrimanis, K.; Nikolakakis, I.; Malamataris, S., Spherical crystal agglomeration of ibuprofen by the solvent-change technique in presence of methacrylic polymers. *J Pharm Sci* **2000,** *89* (2), 250-259.

26. Ahmed, T. A., Preparation of finasteride capsules-loaded drug nanoparticles: formulation, optimization, in vitro, and pharmacokinetic evaluation. *Int J Nanomed* **2016,** *11*.

27. Di Martino, P.; Scoppa, M.; Joiris, E.; Palmieri, G. F.; Andres, C.; Pourcelot, Y.; Martelli, S., The spray drying of acetazolamide as method to modify crystal properties and to improve compression behaviour. *Int J Pharmaceut* **2001,** *213* (1-2), 209-221.

28. Kasa, P.; Bajdik, J.; Zsigmond, Z.; Pintye-Hodi, K., Study of the compaction behaviour and compressibility of binary mixtures of some pharmaceutical excipients during direct compression. *Chem Eng Process* **2009,** *48* (4), 859-863.

29. Kaialy, W.; Larhrib, H.; Chikwanha, B.; Shojaee, S.; Nokhodchi, A., An approach to engineer paracetamol crystals by antisolvent crystallization technique in presence of various additives for direct compression. *Int J Pharmaceut* **2014,** *464* (1-2), 53-64.

30. Lamesic, D.; Planinsek, O.; Lavric, Z.; Ilic, I., Spherical agglomerates of lactose with enhanced mechanical properties. *Int J Pharmaceut* **2017,** *516* (1-2), 247-257.

31.   Nokhodchi, A.; Maghsoodi, M., Preparation of spherical crystal agglomerates of naproxen containing disintegrant for direct tablet making by spherical crystallization technique. *Aaps Pharmscitech* **2008,** *9* (1), 54-59.

32.   Rasenack, N.; Muller, B. W., Crystal habit and tableting behavior. *Int J Pharmaceut* **2002,** *244* (1-2), 45-57.

33.   Mira Jivraj, L. G. M. a. C. M. T., An overview of the different excipients useful for the direct compression of tablets. *Pharm Sci Technolo Today* **2000,** *3* (2), 59-63.

34.   Nokhodchi, A.; Bolourtchian, N.; Dinarvand, R., Crystal modification of phenytoin using different solvents and crystallization conditions. *Int J Pharmaceut* **2003,** *250* (1), 85-97.

35.   Nikolakakis, I.; Kachrimanis, K.; Malamataris, S., Relations between crystallisation conditions and micromeritic properties of ibuprofen. *Int J Pharmaceut* **2000,** *201* (1), 79-88.

36.   Abd-Elbary, A.; Haider, M.; Sayed, S., In vitro characterization and release study of Ambroxol hydrochloride matrix tablets prepared by direct compression. *Pharm Dev Technol* **2012,** *17* (5), 562-573.

37.   Ingredients, B. P., *Generic Drug Formulations*. 2004.

38.   Peralta, J.; Poderoso, J. J.; Corazza, C.; Fernandez, M.; Guerreiro, R. B.; Wiemeyer, J. C. M., Ambroxol Plus Amoxicillin in the Treatment of Exacerbations of Chronic-Bronchitis. *Arzneimittel-Forsch* **1987,** *37-2* (8), 969-971.

39.   Ren, Y. C.; Wang, L.; He, H. B.; Tang, X., Pulmonary Selectivity and Local Pharmacokinetics of Ambroxol Hydrochloride Dry Powder Inhalation in Rat. *J Pharm Sci-Us* **2009,** *98* (5), 1797-1803.

40.   Yamaya, M.; Nishimura, H.; Nadine, L. K.; Ota, C.; Kubo, H.; Nagatomi, R., Ambroxol inhibits rhinovirus infection in primary cultures of human tracheal epithelial cells. *Arch Pharm Res* **2014,** *37* (4), 520-529.

41.   Oxford, J. S.; Leuwer, M., Acute sore throat revisited: clinical and experimental evidence for the efficacy of over-the-counter AMC/DCBA throat lozenges. *Int J Clin Pract* **2011,** *65* (5), 524-530.

42.   Kawashima, Y., Spherical Crystallization and Pharmaceutical Systems. *Pharm Int* **1984,** *5* (2), 40-43.

43.   Jain, A.; Jain, A.; Jain, A.; Jain, A., Quasi emulsion spherical crystallization technique based environmentally responsive Tulsion (R) (pH dependent) microspheres for colon specific delivery. *J Appl Biomed* **2016,** *14* (2), 147-155.

44.   Espitalier, F.; Biscans, B.; Laguerie, C., Particle design Part B: batch quasi-emulsion process and mechanism of grain formation of ketoprofen. *Chem Eng J* **1997,** *68* (2-3), 103-114.

45.   Sano, A.; Kuriki, T.; Kawashima, Y.; Takeuchi, H.; Hino, T.; Niwa, T., Particle Design for Antidiabetic Drugs by the Spherical Crystallization Technique .4. Assessment of Compressibility of Agglomerated Tolbutamide Crystals Prepared by Crystallization Technique. *Chem Pharm Bull* **1992,** *40* (6), 1573-1581.

46.   Sonoda, T.; Takata, Y.; Ueno, S.; Sato, K., Effects of emulsifiers on crystallization behavior of lipid crystals in nanometer-size oil-in-water emulsion droplets. *Cryst Growth Des* **2006,** *6* (1), 306-312.

47.   Kawashima, Y.; Fude, C.; Takeuchi, H.; Niwa, T.; Hino, T.; Kihara, K., Agglomeration Behavior and Modification of Spherical Crystallization Process of Pharmaceuticals by the Emulsion-Solvent-Diffusion Method and Proposed Closed-Circuit Batch System. *Yakugaku Zasshi* **1991,** *111* (8), 451-462.

48.   Nocent, M.; Bertocchi, L.; Espitalier, F.; Baron, M.; Couarraze, G., Definition of a solvent system for spherical crystallization of salbutamol sulfate by quasi-emulsion solvent diffusion (QESD) method. *J Pharm Sci* **2001,** *90* (10), 1620-1627.

49.   Iqbal, J.; Ulrich, J., Spherical particle generation by phase change materials: Near monosize particles from emulsions. *Chem Eng Technol* **2010,** *33* (6), 1011-1014.

50.   Yang, M.; Cui, F.; Fan, Y.; You, B.; Ren, K.; Feng, H.; Kawashima, Y., Effect of three types of additives in poor solvent on preparation of sustained-release nitrendipine microspheres by the quasi-emulsion solvent diffusion method. *J Drug Deliv Sci Tec* **2005,** *15* (2), 129-135.

51.   Re, M. I.; Biscans, B., Preparation of microspheres of ketoprofen with acrylic polymers by a quasi-emulsion solvent diffusion method. *Powder Technol* **1999,** *101* (2), 120-133.

52.   Morishima, K.; Kawashima, Y.; Kawashima, Y.; Takeuchi, H.; Niwa, T.; Hino, T., Micromeritic Characteristics and Agglomeration Mechanisms in the Spherical Crystallization of Bucillamine by the Spherical Agglomeration and the Emulsion Solvent Diffusion Methods. *Powder Technol* **1993,** *76* (1), 57-64.

53.   Fodor-Kardos, A.; Toth, J.; Gyenis, J., Preparation of protein loaded chitosan microparticles by combined precipitation and spherical agglomeration. *Powder Technol* **2013,** *244*, 16-25.

54.   Nowee, S. M.; Abbas, A.; Romagnoli, J. A., Model-based optimal strategies for controlling particle size in antisolvent crystallization operations. *Cryst Growth Des* **2008,** *8* (8), 2698-2706.

55.   Sano, A.; Kuriki, T.; Kawashima, Y.; Takeuchi, H.; Hino, T.; Niwa, T., Particle Design of Tolbutamide by the Spherical Crystallization Technique .3. Micromeritic Properties and Dissolution Rate of Tolbutamide Spherical Agglomerates Prepared by the Quasi-Emulsion Solvent Diffusion Method and the Solvent Change Method. *Chem Pharm Bull* **1990,** *38* (3), 733-739.

56.   Solomatov, V. S., Batch Crystallization under Continuous Cooling - Analytical Solution for Diffusion-Limited Crystal-Growth. *J Cryst Growth* **1995,** *148* (4), 421-431.

57.   Nagy, Z. K.; Chew, J. W.; Fujiwara, M.; Braatz, R. D., Comparative performance of concentration and temperature controlled batch crystallizations. *J Process Contr* **2008,** *18* (3-4), 399-407.

58.   Nagy, Z. K.; Fujiwara, M.; Woo, X. Y.; Braatz, R. D., Determination of the kinetic parameters for the crystallization of paracetamol from water using metastable zone width experiments. *Ind Eng Chem Res* **2008,** *47* (4), 1245-1252.

59.   Abioye, A. O.; Chi, G. T.; Simone, E.; Nagy, Z., Real-time monitoring of the mechanism of ibuprofen-cationic dextran crystanule formation using crystallization process informatics system (CryPRINS). *Int J Pharmaceut* **2016,** *509* (1-2), 264-278.

60.   Markovits, I.; Farkas, B.; Farkas, J.; Rona, P.; Rausz, V.; Jani-Vakulya, G.; Nagy, K., Process Optimization of Filling Up Crystallization. *Chem Eng Technol* **2010,** *33* (5), 845-850.

61.   Saleemi, A. N.; Rielly, C. D.; Nagy, Z. K., Monitoring of the combined cooling and antisolvent crystallisation of mixtures of aminobenzoic acid isomers using ATR-UV/vis spectroscopy and FBRM. *Chem Eng Sci* **2012,** *77*, 122-129.

62.   Katta, J.; Rasmuson, A. C., Spherical crystallization of benzoic acid. *Int J Pharmaceut* **2008,** *348* (1-2), 61-69.

63.   Aamir, E.; Nagy, Z. K.; Rielly, C. D., Optimal seed recipe design for crystal size distribution control for batch cooling crystallisation processes. *Chem Eng Sci* **2010,** *65* (11), 3602-3614.

64.   Wang, X.; Gillian, J. M.; Kirwan, D. J., Quasi-emulsion precipitation of pharmaceuticals. 1. Conditions for formation and crystal nucleation and growth behavior. *Cryst Growth Des* **2006,** *6* (10), 2214-2227.

65.   Burger, A.; Griesser, U. J., Physical Stability, Hygroscopicity and Solubility of Succinylsulfathiazole Crystal Forms - the Polymorphic Drug Substances of the European Pharmacopoeia .7. *Eur J Pharm Biopharm* **1991,** *37* (2), 118-124.

66.   Kumar, G. M.; Cheruvu, S. H.; Sujatha, D.; Sampathi, S., Formulation and Characterization of Ambroxol Hydrochloride Loaded Ethyl Cellulose Microparticles for Sustained Release. *J Biomater Tiss Eng* **2014,** *4* (9), 669-678.

67.   ICH Q8(R2) Guidance for Industry Q8(R2) Pharmaceutical Development. **2009**.

68.   ICH Q9, 2006. Quality Risk Management Guidance for Industry. **2006**.

69.   Kovacs, A.; Berko, S.; Csanyi, E.; Csoka, I., Development of nanostructured lipid carriers containing salicyclic acid for dermal use based on the Quality by Design method. *Eur J Pharm Sci* **2017,** *99*, 246-257.

70.   Kirrstetter, R., GMP aspects in practice: The new ICH guidelines concerning quality: ICH Q8, Q9 and Q10. *Pharm Ind* **2005,** *67* (2), 213-216.

71.   Juran, J. M., The Quality Trilogy. *Qual Prog* **1986,** *19* (8), 19-24.

72.   Hales, D.; Vlase, L.; Porav, S. A.; Bodoki, A.; Barbu-Tudoran, L.; Achim, M.; Tamuta, L., A quality by design (QbD) study on enoxaparin sodium loaded polymeric microspheres for colon-specific delivery. *Eur J Pharm Sci* **2017,** *100*, 249-261.

73.   Beirao-da-Costa, S.; Duarte, C.; Moldao-Martins, M.; Beirao-da-Costa, M. L., Physical characterization of rice starch spherical aggregates produced by spray-drying. *J Food Eng* **2011,** *104* (1), 36-42.

74.   Paradkar, A. R.; Pawar, A. P.; Chordiya, J. K.; Patil, V. B.; Ketkar, A. R., Spherical crystallization of celecoxib. *Drug Dev Ind Pharm* **2002,** *28* (10), 1213-1220.

75.   Wang, J. L.; Kan, S. L.; Chen, T.; Liu, J. P., Application of quality by design (QbD) to formulation and processing of naproxen pellets by extrusion-spheronization. *Pharm Dev Technol* **2015,** *20* (2), 246-256.

76.   Pallagi, E.; Ambrus, R.; Szabo-Revesz, P.; Csoka, I., Adaptation of the quality by design concept in early pharmaceutical development of an intranasal nanosized formulation. *Int J Pharmaceut* **2015,** *491* (1-2), 384-392.

77.   Karimi, K.; Pallagi, E.; Szabo-Revesz, P.; Csoka, I.; Ambrus, R., Development of a microparticle-based dry powder inhalation formulation of ciprofloxacin hydrochloride applying the quality by design approach. *Drug Des Dev Ther* **2016,** *10*, 3331-3343.

78.   Zhang, Y.; Jiang, Y. B.; Zhang, D. K.; Qian, Y.; Wang, X. Z., Metastable zone width, crystal nucleation and growth kinetics measurement in anti-solvent crystallization of beta-artemether in the mixture of ethanol and water. *Chem Eng Res Des* **2015,** *95*, 187-194.

79.   Raphael, M.; Rohani, S., On-line estimation of solids concentrations and mean particle size using a turbidimetry method. *Powder Technol* **1996,** *89* (2), 157-163.

80.   Kempkes, M.; Eggers, J.; Mazzotti, M., Measurement of particle size and shape by FBRM and in situ microscopy. *Chem Eng Sci* **2008,** *63* (19), 4656-4675.

81.   Ruf, A.; Worlitschek, J.; Mazzotti, M., Modeling and experimental analysis of PSD measurements through FBRM. *Part Part Syst Char* **2000,** *17* (4), 167-179.
82.   Farquharson, S.; Charpenay, S.; DiTaranto, M. B.; Rosenthal, P. A.; Zhu, W.; Pratsinis, S. E., In-situ particle size and shape analysis during flame synthesis of nanosize powders. *Acs Sym Ser* **1998,** *681*, 170-186.
83.   Barrett, P.; Glennon, B., In-line FBRM monitoring of particle size in dilute agitated suspensions. *Part Part Syst Char* **1999,** *16* (5), 207-211.
84.   Simon, L. L.; Nagy, Z. K.; Hungerbuhler, K., Comparison of external bulk video imaging with focused beam reflectance measurement and ultra-violet visible spectroscopy for metastable zone identification in food and pharmaceutical crystallization processes. *Chem Eng Sci* **2009,** *64* (14), 3344-3351.
85.   Nordstrom, F. L.; Rasmuson, A. C., Solubility and melting properties of salicylamide. *J Chem Eng Data* **2006,** *51* (5), 1775-1777.
86.   Toldy, A. I.; Badruddoza, A. Z. M.; Zheng, L.; Hatton, T. A.; Gunawan, R.; Rajagopaan, R.; Khan, S. A., Spherical Crystallization of Glycine from Monodisperse Microfluidic Emulsions. *Cryst Growth Des* **2012,** *12* (8), 3977-3982.
87.   Griffin, W. C., Classification of Surface-Active Agents by 'HLB'. *Journal of the Society of Cosmetic Chemists* **1949,** *1* (5), 311-326.
88.   Gyulai, O.; Szabo-Reyesz, P.; Aigner, Z., Comparison Study of Different Spherical Crystallization Methods of Ambroxol Hydrochloride. *Cryst Growth Des* **2017,** *17* (10), 5233-5241.
89.   Hartung, A.; Johansson, E.; Knoell, M.; Valthorsson, H.; Langguth, P., "Design Space" Determination of a Paracetamol Fluid Bed Granulation Using Design of Experiments. *Pharm Ind* **2012,** *74* (4), 644-650.
90.   Iurian, S.; Turdean, L.; Tomuta, I., Risk assessment and experimental design in the development of a prolonged release drug delivery system with paliperidone. *Drug Des Dev Ther* **2017,** *11*, 733-746.
91.   Casian, T.; Iurian, S.; Bogdan, C.; Rus, L.; Moldovan, M.; Tomuta, I., QbD for pediatric oral lyophilisates development: risk assessment followed by screening and optimization. *Drug Dev Ind Pharm* **2017,** *43* (12), 1932-1944.
92.   Reddy, P. R. V.; Acharya, S. R.; Acharya, N. S., Optimization of size controlled poly (lactide-co-glycolic acid) nanoparticles using quality by design concept. *Asian J Pharm* **2015,** *9* (3), 152-161.
93.   Vilfredo Pareto, A. N. P., *Translation of Manuale di economia politica ("Manual of political economy")*. A.M. Kelley: 1971.
94.   O'Ciardha, C. T.; Hutton, K. W.; Mitchell, N. A.; Frawley, P. J., Simultaneous Parameter Estimation and Optimization of a Seeded Antisolvent Crystallization. *Cryst Growth Des* **2012,** *12* (11), 5247-5261.
95.   Power, G.; Hou, G. Y.; Kamaraju, V. K.; Morris, G.; Zhao, Y.; Glennon, B., Design and optimization of a multistage continuous cooling mixed suspension, mixed product removal crystallizer. *Chem Eng Sci* **2015,** *133*, 125-139.
96.   Litten, D. Project Risk and Risk Management. https://pmhut.com/project-risk-and-risk-management.
97.   Box, G. E. H., W. G.; Hunter, J. S. , Statistics for Experimenters: Design, Innovation, and Discovery (2nd ed.). Wiley. ISBN 0-471-71813-0. **2005**.
98.   Orsolya Gyulai, A. K., Tamás Sovány, Ildikó Csóka, Zoltán Aigner, Optimization of the Critical Parameters of the Spherical Agglomeration Crystallization Method by the Application of the Quality by Design Approach. *Materials* **2018,** *11(4)* (635).

99.   Medicines, E. D. f. Q. o., Test for extractable volume of parenteral preparations. In *European Pharmacopoeia*, Strasbourg, 2005; pp 242-243.

100.   Sovany, T.; Kasa, P.; Pintye-Hodi, K., Modeling of Subdivision of Scored Tablets with the Application of Artificial Neural Networks. *J Pharm Sci-Us* **2010,** *99* (2), 905-915.

101.   Patra, C. N.; Swain, S.; Mahanty, S.; Panigrahi, K. C., Design and characterization of aceclofenac and paracetamol spherical crystals and their tableting properties. *Powder Technol* **2015,** *274*, 446-454.

102.   ICH Harmonized Guideline Impurities: Guideline for Residual Solvents Q3C(R6) In *Q3C(R6)* 4th ed., **2016**

103.   Pingali, K. C.; Saranteas, K.; Foroughi, R.; Muzzio, F. J., Practical methods for improving flow properties of active pharmaceutical ingredients. *Drug Dev Ind Pharm* **2009,** *35* (12), 1460-1469.

104.   Shaikh, K. A.; Patil, S. D.; Devkhile, A. B., Development and validation of a reversed-phase HPLC method for simultaneous estimation of ambroxol hydrochloride and azithromycin in tablet dosage form. *J Pharmaceut Biomed* **2008,** *48* (5), 1481-1484.

105.   Gowekar, N. M.; Pande, V. V.; Kasture, A. V.; Tekade, A. R.; Chandorkar, J. G., Spectrophotometric Estimation of Ambroxol and Cetirizine Hydrochloride from Tablet Dosage Form. *Pak J Pharm Sci* **2007,** *20* (3), 249-250.

106.   Indrayanto, G.; Handayani, R., Quantitative-Determination of Ambroxol Hydrochloride in Tablets. *J Pharmaceut Biomed* **1993,** *11* (8), 781-784.

107.   Vujovic, M. M.; Jokanovic, M.; Nikolic, G. M., In vitro dissolution profile study of mucolytic drug ambroxol hydrochloride from solid oral dosage form by UHPLC-MS/MS. *Hem Ind* **2017,** *71* (1), 75-83.

108.   DFE Pharma, Introduction to tableting by direct compression. Accessible: https://www.dfepharma.com/en/knowledge-base/oral-solid-dose/direct-compression.aspx, 2018.05.29.

NYILATKOZAT SAJÁT MUNKÁRÓL

Név: Gyulai Orsolya

A doktori értekezés címe: Development of directly compressible ambroxol hydrochloride spherical crystals

Én, Gyulai Orsolya teljes felelősségem tudatában kijelentem, hogy a Szegedi Tudományegyetem Gyógyszertudományok Doktori Iskolában elkészített doktori (Ph.D.) disszertációm saját kutatási eredményeimen alapulnak. Kutatómunkám, eredményeim publikálása, valamint disszertációm megírása során a Magyar Tudományos Akadémia Tudományetikai Kódexében lefektetett alapelvek és ajánlások szerint jártam el.

Szeged, 2018. 05. 29.

_____